学位論文

Analysis of Cortical Actin Microfilaments in Determination of Plant Cell Division Plane

（高等植物の細胞分裂面決定における表層アクチン繊維のイメージング解析）

平成 25 年 12 月博士（生命科学）申請

東京大学大学院新領域創成科学研究科

先端生命科学専攻

湖城 恵

Analysis of Cortical Actin Microfilaments in Determination of Plant Cell Division Plane

Kei Kojo

2013

Department of Integrated Biosciences,

Graduate School of Frontier Sciences,

The University of Tokyo

Acknowledgments

I first with to express my deepest appreciation to Prof. Seiichiro Hasezawa (The University of Tokyo) for his guidance and encouragement throughout this study.

I am also grateful to Dr. Natsumaro Kutsuna (The University of Tokyo) and Dr. Takumi Higaki (The University of Tokyo) for their instructions and critical suggestions.

I am grateful to Dr. Hiroki Yasuhara (Kansai University) for the kind gift of BY-YTRF cells. I thank to Mr. Yuya Yoshida (The University of Tokyo) for experimental support of microscopic observation. I thank to Ms. Yukari Hamada (The University of Tokyo) for critical suggestions regarding *Arabidopsis* growth conditions.

I want to thank all of the members of the Laboratory of Plant Cell Biology in Totipotency for their help and encouragement. Finally, I want to thank my family and friends for their continuous support through this study.

Contents

Abbreviations

2,4-D: 2,4-dichlorophenoxyacetic acid

ABD2: actin-binding domain 2 of *Arabidopsis* fimbrin 1

ADD1: alternate discordia1

BY-2: Bright Yellow 2

BY-GF11: transgenic BY-2 cell line stably expressing GFP-ABD2 fusion protein clone 11

BY-GT16: transgenic BY-2 cell line stably expressing GFP-tubulin fusion protein clone 16

BY-YTRF1: transgenic BY-2 cell line stably expressing YFP-tubulin fusion protein and RFP (tdTomato)-ABD2 fusion protein clone 1

CCD: charge coupled device

DCD1: discordia1

DMSO: dimethyl sulfoxide

FM4-64:

N-(3-triethylammoniumpropyl)-4-(6-(4-(diethylamino)-phenyl)hexatrienyl)pyridinium dibromide

GFP: green fluorescent protein

IQR: interquartile range

LS: Linsmaier and Skoog

mTn: mouse talin

PIP2a: plasma membrane intrinsic protein 2a

PMEG: polyethylene glycol

RFP: red fluorescent protein

TIBA: 2,3,5-triiodobenzonic acid

YFP: yellow fluorescent protein

Abstract

In land plant cells, division planes are precisely predicted by the microtubule preprophase band and cortical actin microfilament pattern called actin-depleted zone or actin microfilament twin peaks. However, the function of cortical actin microfilament patterning is not clear. Treatment with the inhibitor 2,3,5-triiodobenzonic acid (TIBA) or jasplakinolide increased the amount of thick actin microfilaments in tobacco BY-2 cells at interphase. However, during the division of BY-2 cells, these inhibitors did not induce visible alteration of actin microfilament thickness but altered cortical actin microfilament patterning without significant disorganization of the microtubule preprophase band. TIBA treatment induced a single intensity peak of actin microfilament distribution around the cell center, whereas jasplakinolide caused the appearance of triple peaks relative to the distribution of actin microfilament around the cell center, in approximately one-third of the cells at metaphase. Dual observations of microtubules and actin microfilaments revealed that abnormal cortical actin microfilament patterning with single or triple peaks is correlated with oblique mitotic spindles in BY-2 cells. In addition, oblique cell plates were frequently observed in BY-2 cells and *Arabidopsis thaliana* root cells treated with TIBA or jasplakinolide. These results provide evidence for the critical roles of cortical actin microfilament patterning on spindle and cell plate orientation (Kojo et al. 2013).

Introduction

Orientation of the cell division plane is crucial for the plant body plan because plant cells possess a rigid cell wall. The division plane site depends on spindle and phragmoplast positioning during mitosis, and proper spindle orientation facilitates phragmoplast positioning and orientation (Granger and Cyr 2001; Yoneda et al. 2005). In land plants, division planes are precisely predicted by a ring of cortical microtubules called the preprophase band, which originates as a wide microtubule ring then narrows to mature in late G2 phase and ultimately disappears at the transition from prophase to metaphase (Mineyuki 1999). Actin microfilaments have also been postulated to contribute to the determination of division plane orientation (Panteris 2008). After the preprophase band disappears, cortical actin microfilaments become sparse in the future cortical division site during metaphase and form an actin-depleted zone (Cleary et al. 1992; Liu and Palevitz 1992). The cortical division site is positively marked by the preprophase band at late G2 phase, and thereafter negatively marked by the actin-depleted zone from metaphase to cytokinesis (Hoshino et al. 2003). The presence of the actin-depleted zone has been confirmed in several plant species and cell types (Panteris 2008). However, high resolution imaging studies demonstrated that cortical actin microfilaments were not completely depleted even in the actin-depleted zone (Hoshino et al. 2003; Valster et al. 1997). A series of live cell imaging also showed that many actin microfilaments were present in the actin-depleted zone and that a dense actin microfilament

meshwork emerged on either side of the actin-depleted zone in a transgenic tobacco BY-2 cell line stably expressing a GFP-ABD2 fusion protein, designated BY-GF11 (Higaki et al. 2007; Higaki et al. 2008; Sano et al. 2005). The actin microfilament density gradient was considered as important in division plane orientation and named the distribution as actin microfilament 'twin peaks' in BY-2 cells (Sano et al. 2005; Higaki et al. 2008). Obviously, actin-depleted zone and actin microfilament twin peaks are inextricably linked to each other; however, here, I use the term actin microfilament twin peaks because I focused on the changes in the peaks relative to actin microfilament distribution.

It was reported that treatment of bistheonellide A or cytochalasin D, actin polymerization inhibitors, induces oblique cell plate formation, suggesting that actin microfilament twin peaks function in division plane orientation (Hoshino et al. 2003; Sano et al. 2005). However, these actin polymerization inhibitors completely disrupt actin microfilaments, and therefore the significance of the distributional patterns cannot be examined using these inhibitors. In addition, actin microfilament disruption occasionally causes secondary effects on microtubules because of the close association between microtubules and actin microfilaments (Mineyuki and Palevitz 1990; Sampathkumar et al. 2011). It was reported that treatment with actin polymerization inhibitors also secondarily inhibits preprophase band narrowing (Mineyuki 1999; Mineyuki and Palevitz 1990). Currently,

therefore, there is no direct evidence for the role of actin microfilament twin peaks in division plane orientation.

The identification and use of less disruptive agents for examining the significance of actin microfilament twin peaks have long been awaited. Recently, 2,3,5-triiodobenzonic acid (TIBA), an auxin transport inhibitor (Geldner et al. 2001; Kleine-Vehn et al. 2006; Niedergang-Kamien and Leopold 1957; Snyder 1949) was reported to affect actin microfilament organization in non-dividing yeast, mammalian and plant cells (Dhonukshe et al. 2008). Jasplakinolide, an actin targeting peptide, enhanced actin microfilament polymerization by inhibiting actin depolymerization activity, especially at low concentrations and for short exposure times in plant and animal cells (Bubb et al. 1994; Ou et al. 2002; Spector et al. 1999). However, these studies focused on the inhibitory effects on non-dividing cells, while their effects on dividing plant cells have not yet been examined.

Here, I found that treatment with TIBA and jasplakinolide altered actin microfilament twin peaks patterning without significant effects on microtubule preprophase band organization in tobacco BY-2 cells and resulted in an oblique division plane. Dual observations of microtubules and actin microfilaments revealed that the disordered actin microfilament twin peaks pattern is correlated with an oblique mitotic spindle orientation. Time sequential observation of cortical actin microfilaments and division plane orientation revealed that disordered actin microfilament twin peaks resulted in an oblique phragmoplast

and division plane following an oblique mitotic spindle. These results support a critical role of actin microfilament twin peaks in division plane orientation.

Materials and Methods

Plant material

Tobacco BY-2 (*Nicotiana tabacum* L. cv. Bright Yellow 2) suspensions were diluted 95-fold with modified Linsmaier and Skoog (LS) medium supplemented with 2,4-D at weekly intervals, as previously described (Nagata et al. 1992). The cell suspensions were agitated on a rotary shaker at 130 rpm at 27°C in the dark. Cell synchronization was performed as previously described (Kumagai-Sano et al. 2006). In brief, 3 mL of 7-day-old cells were transferred into 30 mL fresh medium and cultured for 24 h with 5 mg L^{-1} aphidicolin (Sigma, St Louis, MO, USA). The cells were washed with 10 volumes of fresh medium and then resuspended in the same medium.

A transgenic BY-2 cell line, stably expressing a GFP-tubulin fusion protein, was established and designated BY-GT16 as previously described (Kumagai et al. 2001). The BY-GF11 cell line, which stably expresses a GFP-ABD2 fusion protein, was also established as previously described (Sano et al. 2005). The BY-YTRF1 cell line, which stably expressing YFP-tubulin fusion protein and tdTomato-ABD2 fusion protein, was also established as previously described (Kojo et al. 2013). These cell lines could be maintained and synchronized by similar procedures used for the original BY-2 cell line.

Microscopy

For time-sequential observations, BY-GF11, BY-GT16, and BY-YTRF1 lines were transferred into 35-mm-diameter Petri dishes with 14-mm-diameter coverslip windows at the bottom (Matsunami Glass Ind. Ltd., Osaka, Japan). The dishes were placed onto the inverted platform of a fluorescence microscope (IX-71: Olympus, Tokyo, Japan) equipped with a confocal scanning unit (CSU 10, Yokogawa, Tokyo, Japan) and a cooled CCD camera (Cool-SNAP HQ or Cool-SNAP HQ2, PhotoMetrics, Huntington Beach, Canada). Maximum intensity projection images were constructed from the serial optical sections within a 0.5 μm step size using METAMORPH software (Universal Imaging, Downingtown, PA, USA). The images were processed digitally using ImageJ software (Abramoff et al. 2004).

Inhibitor treatment

To disrupt actin microfilament, 7-day-old BY-2 cells or synchronized BY-2 cells were treated with 2 μM latrunculin B for 30 min to 5 h at 27°C. To modify actin microfilament organization, 7-day-old BY-2 cells or synchronized BY-2 cells were treated with 5 μM TIBA or 30 nM jasplakinolide for 30 min to 5 h at 27°C. As a control, the cells were treated with an equal volume of dimethyl sulfoxide (DMSO) for 30 min to 5 h at 27°C.

Cell staining

To observe the vacuolar membrane and plasma membrane in BY-GF11 cells, N-(3-triethylammoniumpropyl)-4-(6-(4-(diethylamino)-phenyl)hexatrienyl)pyridinium dibromide (FM4-64; Molecular Probes, Invitrogen) was added to the cell suspensions to a final concentration of 3.3 μM. The cells were incubated for 2 h at room temperature and then observed.

To observe the division plane, where the cell plates joined the parental cell walls, early G1 phase cells were fixed with 3.7% (w/v) formaldehyde dissolved in PMEG buffer for 1 h, at 27°C, and stained with 0.05% aniline blue (Biosupplies Australia, Parkville, Victoria, Australia). Subsequently, the cells were observed by fluorescent microscopy (BX51, Olympus).

Measurement of fluorescent intensity

In direct quantification of fluorescent intensity was performed using JAVA plug-in; KBI plug-in for ImageJ. This plug-in package can be downloaded for free from http://hasezawa.ib.k.u-tokyo.ac.jp/zp/Kbi/ImageJKbiPlugins.

Evaluation of GFP-ABD2 fluorescent intensity distribution and skewness

For pre-processing, the outer layer of the cells was manually segmented and actin microfilaments were extracted via band-pass filtering using the KBI plug-in package. To

evaluate the GFP-ABD2 fluorescent intensity distribution, the extracted actin microfilament images were skeletonized using KBI plug-in package and the number of each intensity pixel was counted. The skewness is defined by

$$skewness = \frac{1}{N}\sum_{i=1}^{N}\left(\frac{i_n - \bar{i}}{\sigma}\right)^3$$

$$\sigma = \frac{1}{N}\sum_{i=1}^{N}(i_n - \bar{i})^2$$

where, N , i_n and $\bar{i}$ are the actin microfilament pixel numbers of the skeletonized image, intensity of actin microfilament pixel, and mean intensity of actin microfilament pixel, respectively (Higaki et al. 2010).

Results

Dual observation of characteristic microtubule and actin microfilament structures using BY-YTRF1 cells

To monitor microtubules and actin microfilaments simultaneously in living cells, I used transgenic tobacco BY-2 cell line stably expressing YFP-tubulin and RFP(tdTomato)-ABD2, designated as BY-YTRF1 cells. These cells showed similar growth rates and cell cycle progression to the original BY-2 cells following aphidicolin treatment (Fig. S1). In BY-YTRF1 cells, both microtubules and actin microfilaments could be clearly visualized during cell cycle progression (Kojo et al. 2013). As representative mitotic cytoskeletal structures, the preprophase band from late G2- to prophase (Fig. S2a, c), cortical actin microfilament patterning called actin-depleted zone or actin microfilament twin peaks from prometa- to metaphase (Fig. S2e, f), the mitotic spindle from meta- to anaphase (Fig. S2d, f) and the phragmoplast at telophase could be observed (Fig. S2g-i). These experiments confirmed that BY-YTRF1 cells could be used to observe cytoskeletal components during cell cycle progression.

Time-lapse imaging from pro- to metaphase showed that the preprophase band was formed at the center of the cell cortex in prophase and was disassembled by metaphase (Fig. 1a, b). In metaphase, actin microfilament twin peaks were clear at the cell cortex (Fig. 1b). Measurements of YFP-tubulin and tdTomato-ABD2 fluorescence intensities along the cell cortex indicated that

the actin microfilament twin peaks were formed around the region where the preprophase band was assembled (Fig. 1b, d, e). These results confirmed that BY-YTRF1 cells allowed the simultaneous observation of mitotic microtubule and actin microfilament components.

Preprophase band formation is not altered by TIBA and jasplakinolide

The effects of TIBA and jasplakinolide on the width of the preprophase band were evaluated (Fig. 2). Narrowing of the preprophase band, which originated as a wide microtubule ring, was followed using transgenic tobacco BY-2 cells stably expressing GFP-tubulin (Kumagai et al. 2001). In the case of the latrunculin B treatment, a broad preprophase band was frequently observed even at prophase, suggesting that latrunculin B inhibited preprophase band narrowing (Fig. 2b) as previously reported (Mineyuki 1999; Mineyuki and Palevitz 1990). In the case of TIBA and jasplakinolide treatment, morphologically normal and mature preprophase band were observed (Fig. 2c-d) similar to the DMSO control (Fig. 2a). Measurements of the mature preprophase band width, defined by the full-width at half-maximum of GFP-tubulin fluorescence intensity along the cell cortex line (Fig S3), showed no inhibitory activity of TIBA and jasplakinolide (Fig. 2e). These results indicated that TIBA and jasplakinolide did not induce preprophase band disorganization.

Effects of TIBA and jasplakinolide on cortical actin microfilament patterning at metaphase

The effects of latrunculin B, TIBA and jasplakinolide treatment on the actin microfilament status during cell cycle in BY-GF11 cells were also analyzed. Following latrunculin B treatment, I confirmed that actin microfilaments were disrupted at every phase of the cell cycle (Fig. 3b, f, j, n). I quantitatively evaluated the effects of TIBA and jasplakinolide on actin microfilament status by measuring the skewness of the GFP-ABD2 fluorescent intensity distribution, a numeric indicator of actin bundling level (Higaki et al. 2010). In the cells at G1 phase, similarly to the results reported for *Arabidopsis* guard cells (Higaki et al. 2010), TIBA or jasplakinolide treatment increased the skewness value (Fig. S4), according with the decrease of the relatively gloomy filaments (Fig. S4, arrowheads). These results suggested that thick actin cables become dominant after treatment with TIBA or jasplakinolide following their elimination effects on fine actin microfilaments in BY-2 cells at G1 phase. In addition, I confirmed that TIBA and jasplakinolide increase the frequency thick actin cable in dose-dependent manner at low concentration in the cells at G1 phase (Fig. S5a-c, k-m), although actin microfilaments were severed or disrupted at higher concentration in the cells at G1 phase and metaphase (Fig. S5d, e, i, j, o, t).

Interestingly, however, TIBA- or jasplakinolide-induced dominance of the thick actin cables was not observed at G2 phase or mitotic phase (Fig. 3g, h, k, l, o, p, Fig. S5f-h, p-s) compared with DMSO controls (Fig. 3e, i, m). The values of the skewness also showed no

significant differences on the actin bundling levels (Fig. 3r, s, t), suggesting that influence of these inhibitors on the actin microfilament status was limited to G1 phase.

Although TIBA and jasplakinolide treatment did not alter actin status, they affected distribution patterns of cortical actin microfilaments at metaphase (Fig. 4). At metaphase, more than 90% of cells formed actin microfilament twin peaks, identified as twin intensity peaks of GFP-ABD2 around the center of the cell in DMSO controls (Fig. 4a, d, Table 1), confirming a previous report (Sano et al. 2005). TIBA and jasplakinolide, however, induced different patterns of actin microfilament twin peaks disorganization. TIBA treatment induced a single intensity peak of GFP-ABD2 around the cell center in approximately 37% of cells at metaphase (Fig. 4b, e, Table 1), whereas jasplakinolide caused triple peaks around the cell center in approximately 32% of cells at metaphase (Fig. 4c, f, Table 1). The intensity profiles of GFP-ABD2 fluorescence, obtained by perpendicular signal averaging, clearly showed that cells treated with these inhibitors had altered patterns of cortical actin microfilament distribution (Fig. 4e, f). These results clearly confirm that the TIBA and jasplakinolide specifically perturb actin microfilament twin peaks without affecting preprophase band narrowing.

Changes in actin microfilament distribution on the plasma membrane at metaphase are insensitive to TIBA and jasplakinolide

Actin microfilament patterning at the cell cortex appear to form actin microfilament twin peaks by metaphase, however, it is unclear whether actin microfilament twin peaks are anchored to the plasma membrane or are localized to the vacuolar membrane of the large vacuole. To investigate the detailed localization of actin microfilaments, I visualized the actin microfilament, plasma membrane and vacuolar membrane simultaneously by staining BY-GF11 cells with FM4-64, a styryl dye that labels the vacuolar membrane and plasma membrane (Fig. S6b; Kutsuna and Hasezawa 2002). The vacuolar membrane and plasma membrane regions were then manually selected as line segments from original microscopic images via image processing (Fig. S6b-d), and the mean GFP-ABD2 intensities in the plasma membrane and vacuolar membrane regions were measured (Fig. S6a, e, f). As a quantitative indicator of actin microfilament distribution, the plasma membrane/vacuolar membrane ratio of GFP-ABD2 intensity was employed. Examination of these ratios revealed that actin microfilaments were mainly localized to the vacuolar membrane at G2 phase (Fig. 5a-d, i) but relocated to the plasma membrane at metaphase (Fig. 5e-i). Although TIBA and jasplakinolide induced actin microfilament twin peaks disorganization (Fig. 4), they did not affect this aspect of actin microfilament relocation (Fig. 5j, k, Fig. S7), suggesting that TIBA and jasplakinolide do not inhibit actin microfilament anchoring to the plasma membrane.

TIBA and jasplakinolide treatment resulted in oblique cell plate insertion in BY-2 cells and *Arabidopsis thaliana* root tips

The cell plate angles were examined with aniline blue staining in the cells treated with TIBA and jasplakinolide. As previously reported (Hoshino et al. 2003, Sano et al. 2005), latrunculin B treatment caused an oblique cell plate with an angle of more than 10 degrees in approximately 14% of cells (Fig. 6e, Table S1), even though the cell plate was inserted almost perpendicular to the long axis of cells in DMSO controls (Fig. 6a, Table S1). TIBA and jasplakinolide also caused oblique cell plates with an angle of more than 10 degrees in approximately 20% and 15% of cells, respectively (Fig. 6c-e, Table S1). These results indicate that treatment with TIBA and jasplakinolide resulted in oblique cell plate insertion in BY-2 cells.

To confirm the effects of TIBA and jasplakinolide on cell division plane orientation *in planta*, I observed *Arabidopsis* root tips expressing various GFP fusion proteins. As I was unfortunately unable to obtain clear images of GFP-ABD2 in the *Arabidopsis* root tip, I used transgenic *Arabidopsis* expressing GFP-mouse talin (mTn) (Sano et al. 2005), which allowed us to observe actin microfilaments in the root cortex and which showed normal perpendicular division planes in the gravitational direction (Fig. S8). Actin microfilaments were disrupted in latrunculin B-treated roots (Fig. S8b) but not in DMSO controls, or in TIBA- or jasplakinolide-treated roots (Fig. S8a, c, d). I used transgenic *Arabidopsis* expressing GFP-PIP2a (Cutler et al. 2000) to observe the division plane orientation. Despite the existence of actin

microfilaments, the frequencies of oblique division planes were increased significantly in 1-week-old GFP-PIP2a-expressing *Arabidopsis* root tips treated with TIBA or jasplakinolide for 24 h (Fig. 7c, d, Table. S1) as well as in latrunculin B-treated root tips (Fig. 7b, Table. S1). Latrunculin B, TIBA and jasplakinolide caused oblique division planes with angles of more than 10 degrees in approximately 15%, 13% and 11% of cells, respectively (Fig. 7e). These results support that normal cortical actin microfilament patterning is correlated with proper division plane orientation in root cell division in *Arabidopsis*.

Dual observations of cortical actin microfilament patterning and orientation of mitotic spindles

My results showed that TIBA and jasplakinolide altered cortical actin microfilament patterning at metaphase. The effects of these inhibitors on the orientations of the mitotic spindles and cell plate were evaluated using BY-YTRF1 cells. Treatment with TIBA or jasplakinolide increased the frequency of cells with oblique spindles with angles more than 10 degrees against the cell short axis (Fig. 8a-c, g). To examine the relationship between actin microfilament twin peaks and spindle orientations, cells were classified as cells with normal twin peaks or abnormal single or triple peaks based on the tdTomato-ABD2 fluorescence intensity profiles (Fig. S9). In cells with abnormal cortical actin microfilament patterning with single or triple peaks, oblique mitotic spindles were frequently observed (Fig. 8i, j gray box). It is important to note that even

following treatment with TIBA and jasplakinolide, cells with relatively normal actin microfilament twin peaks possessed normal mitotic spindles (Fig. 8i, j, black box). Conversely, cells with abnormal cortical actin microfilament patterning were observed in fewer than 10% of DMSO control BY-YTRF1 cells as well as BY-GF11 cells (Table 1), and the oblique mitotic spindles were observed in abnormal cells (Fig. 8h gray box). These results indicate that the disordered cortical actin microfilament patterning is correlated with oblique mitotic spindle orientation.

Time sequential observation of cortical actin microfilament patterning and division plane orientation

For further investigation of the relationship between cortical actin microfilament patterning and cell plate orientation, cortical actin microfilaments and orientation of mitotic spindles and the phragmoplasts from metaphase to telophase in BY-YTRF1 cells were observed (Fig. 9). In the cells that possessed altered cortical actin microfilament patterning and an oblique spindle (Fig. 9b, c, Fig. S10b, c), an oblique phragmoplast and an oblique division plane was observed (Fig. 9h, i, k, l, n, o). These results indicate a strong correlation between altered cortical actin microfilament patterning and oblique cell plate orientation in BY-2 cell.

Discussion

Cortical actin microfilament distributions have been postulated to contribute to the regulation of division plane orientation, although the significance of distributional patterns was unclear. In this study, I found that TIBA and jasplakinolide induced alterations of cortical actin microfilament patterning at metaphase. Therefore, I used BY-YTRF1 cell line expressing YFP-tubulin and tdTomato-ABD2 and examined the relationship of cortical actin microfilament patterning and mitotic spindle orientation using dual observation of actin microfilaments and microtubules in living BY-2 cells.

TIBA and jasplakinolide do not induce preprophase band disorganization

In this study, consistent with my observations of the existence of morphologically normal actin microfilaments in the cells treated with TIBA or jasplakinolide at G2 phase (Fig. 3), BY-2 cells treated with TIBA and jasplakinolide appeared to possess normal narrowed preprophase band (Fig. 2). Although Sampathkumar et al. (2011) reported structural associations between microtubules and actin microfilaments, and found that jasplakinolide affected cortical microtubule organization in *Arabidopsis* hypocotyl cells (Sampathkumar et al. 2011), I did not detect any disorganized cortical microtubules or preprophase band in BY-2 cells treated with TIBA or jasplakinolide in G1 phase or late G2 phase. These results imply that the mechanisms of

structural association between microtubules and actin microfilaments vary between species as well as cell type and cell cycle.

TIBA and jasplakinolide do not affect actin microfilament status but do alter actin microfilament patterning during mitosis

It was shown that treatment with TIBA and jasplakinolide could affect actin microfilament status not only in plant cells but also in animal cells (Dhonukshe et al. 2008). However, my results indicated that TIBA and jasplakinolide did not alter actin microfilament status in mitotic BY-2 cells (Fig. 3). I confirmed that treatment with even higher concentrations of these inhibitors did not affect actin microfilament status but did disrupt actin microfilaments at metaphase as previously reported (Ou et al. 2002), suggesting that TIBA and jasplakinolide do not affect actin microfilament status during mitosis at any concentration. Thick actin microfilament is observed at G1 phase, whereas a fine meshwork of actin microfilaments is observed at mitotic phase in BY-GF11 cells (Fig. 3). Therefore, some actin bundling proteins might be down-regulated in mitotic tobacco BY-2 cells. It is possible that TIBA or jasplakinolide remove the fine meshwork of actin microfilaments by stimulating actin bundling protein functions. This idea is supported by *in vitro* experiments, demonstrating purified actin polymerization is not affected by TIBA treatment (Dhonukshe et al. 2008). The mechanistic rationale for which cortical actin microfilament patterning is altered by TIBA and jasplakinolide

treatment is still unclear. Previous reports have shown that these inhibitors induce a defect in actin dynamics (Dhonukshe et al. 2008). Altered actin microfilament patterning may be due to reduced actin dynamics. Future analysis of actin microfilament dynamics will be essential for clarifying this possibility.

Abnormal cortical actin microfilament patterning is correlated with oblique spindle orientation

It was reported that double preprophase bands resulted in an oblique spindle and subsequent cell plate misorientation, suggesting the importance of spindle orientation in division plane orientation in BY-2 cells (Yoneda et al. 2005). In this study, oblique spindle orientation was frequently observed in cells with altered cortical actin microfilament patterning (Fig. 8, Fig. 9). These results suggest that actin microfilament twin peaks play role in spindle positioning for division plane orientation. Although it is conceivable that actin microfilament twin peaks are required for proper actin microfilament organization around the mitotic spindle, I could not detect the visible alternation of actin microfilament organization in TIBA- and jasplakinolide-treated cells (Fig. S7). Furthermore, vacuolar structures showed no differences in TIBA- or jasplakinolide-treated cells (Fig. S7), although actin microfilament disruption did lead to alterations in vacuolar structures as reported previously (Higaki et al. 2006). Thus, the mechanisms that regulate spindle orientation remain unclear at present. In this study, actin

microfilaments were found in metaphase to be closer to the plasma membrane than to the vacuolar membrane, even in cells treated with TIBA or jasplakinolide (Fig. 5j, k), implying that alteration of actin microfilament patterning occur adjacent to the plasma membrane. Actin microfilaments beneath the plasma membrane might be involved in the regulation of spindle and division plane orientation. In AtEB1-GFP expressing cells, microtubules (astral-like microtubules and endoplasmic microtubules) that interact with the cell cortex during mitosis have been reported, and might be involved in the precise establishment of the division plane in *Arabidopsis* and BY-2 cells (Chan et al. 2005; Dhonukshe et al. 2005). Thus, actin microfilament twin peaks adjacent to the plasma membrane may be required for the precise localization of microtubule-anchoring proteins at the cortical division site.

Recent studies have demonstrated the localization of specific proteins to the cortical division site, including TANGLED and RanGAP1 in *Arabidopsis*, and discordia1 (DCD1) and alternate discordia1 (ADD1) in maize (Rasmussen et al. 2010; Walker et al. 2007; Wright et al. 2009; Xu et al. 2008). In this study, the actin microfilaments were found to be closer to the plasma membrane than to the vacuolar membrane in cells treated with TIBA or jasplakinolide (Fig. 5i, j, k), implying that changes in cortical actin microfilament patterning by these inhibitors occur adjacent to the plasma membrane. These results suggest that cortical actin microfilament patterning adjacent to the plasma membrane functions in the regulation of spindle orientation and division planes. In animal and plant cells, the plasma membrane is composed of discrete

membrane domains, such as cholesterol-dependent membrane rafts, which function as specialized signaling platforms in the plasma membrane and are regulated by actin microfilaments adjacent to the plasma membrane (Mongrand et al. 2010). Although a complete picture of membrane and protein components at the cortical division site is still not clear, the actin microfilament twin peaks may play roles in transport and/or retention of membrane proteins at the cortical division site involved in determination of the cell division plane. To investigate the function of cortical actin microfilaments, further studies on identification of membrane protein at the cortical division site and interactions of these protein and cortical actin microfilaments are necessary.

Roles of cortical actin microfilaments in division plane determination in *Arabidopsis thaliana*

Several studies have reported transgenic *Arabidopsis* in which actin microfilaments were labeled with fluorescent proteins, including the GFP-mTn, GFP-ABD2, and GFP-Lifeact (Era et al. 2009; Higaki et al. 2010; Saito et al. 2005). Although cortical actin microfilaments patterning or actin-depleted zones have been observed in symmetrically dividing root cells (Voigot et al., 2005), the importance of cortical actin microfilament patterning in division plane determination in *Arabidopsis* has not yet been confirmed. In this study, I found that treatment with TIBA or jasplakinolide induced an oblique division plane not only in BY-2 cells but also in

Arabidopsis root tips (Fig. 7). I confirmed that these inhibitors do not disrupt actin microfilament organization in the root cortex (FigS. 8). However, I could not detect extra actin bundling in *Arabidopsis* roots, although extra actin bundling was confirmed in epidermal cells, guard cells, and hypocotyl cells treated with these inhibitors. The lack of actin bundling may have resulted from lower GFP expression in the root cortex. Collectively, these results support the importance of cortical actin microfilament patterning in division plane determination in *Arabidopsis* root tips.

In asymmetrically dividing cells of *Zea mays*, actin, particularly the cytoplasmic F-actin cap, plays a role in the migration of the premitotic nucleus into the future division plane (Rasmussen et al., 2011; Panteris et al., 2006; Mineyuki and Palevitz 1990). Additionally, latrunculin B treatment induced misorientation of the phragmoplast in the asymmetrical subsidiary mother cell division, indicating that actin microfilaments play roles in the division plane determination in asymmetrical division in plants (Panteris et al., 2006). In *Arabidopsis*, cortical actin microfilament patterning, such as actin-depleted zone or actin microfilament twin peaks, were observed in the dividing root meristems (Voigt et al 2005). However, actin microfilament pattering has not been reported in asymmetrical dividing tissue such as leaf epidermal cells. Lucas and Sack (2011) reported the occurrence and development of preprophase band formation in a polar fashion in *Arabidopsis* leaf epidermis. To explore the roles of cortical

actin microfilament patterning in asymmetrically dividing cells, temporal and spatial localization analysis of actin microfilaments and microtubules in epidermal cells is necessary.

Conclusion

In land plant cells, division plane is predicted by cortical actin microfilament pattern called actin microfilament twin peaks at metaphase. However, the function of cortical actin microfilament patterning is not clear. In this study, I found that treatment with TIBA and jasplakinolide altered actin microfilament twin peaks patterning. Using these inhibitors, I investigated the relationship between actin microfilament twin peaks and division plane orientation in BY-2 cells.

In conclusion, my observations with TIBA and jasplakinolide suggest that normal cortical actin microfilament distribution recognized as actin microfilament twin peaks is correlated with proper spindle and cell plate orientation. Even when a narrow preprophase band was established, oblique mitotic spindles were frequently observed in cells with disordered cortical actin microfilament patterning at metaphase (Fig. 10). The relationship between the preprophase band and actin microfilament twin peaks is still an open question, but further studies on the roles of actin microfilament twin peaks in the dynamics of preprophase band-localized proteins may shed more light on this issue.

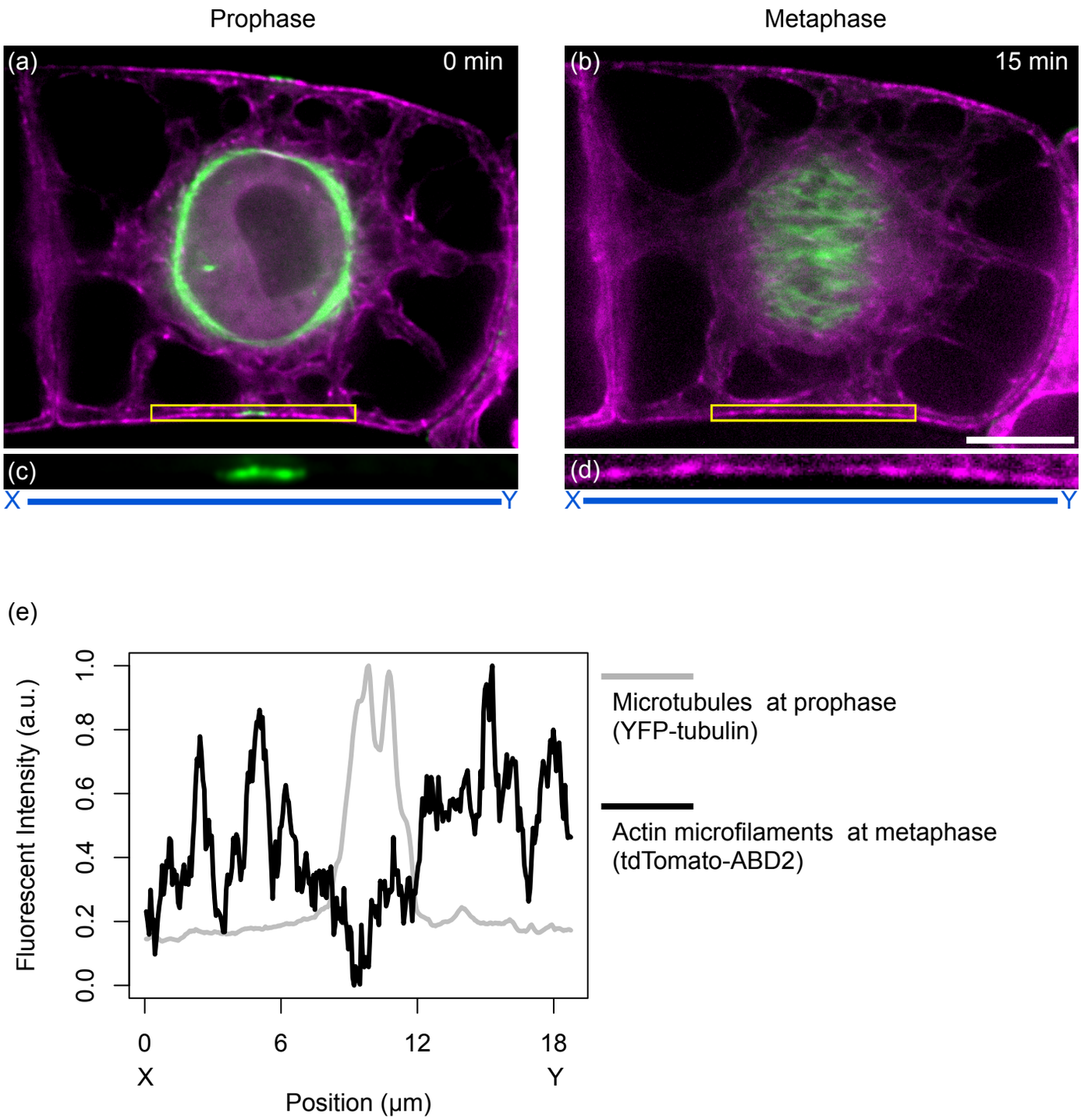

Figure 1. Temporal and spatial relationship between microtubules preprophase band and actin microfilament twin peaks in BY-YTRF1 cells.

(a, b) Time-sequential observations of the microtubules labeled by YFP-tubulin (green) and actin microfilaments labeled by tdTomato-ABD2 (magenta) at prophase (0 min, a) and metaphase (15 min, b). (c) Magnified separated image of the boxed region in (a) of YFP-tubulin fluorescence. (d) Magnified separated image of the boxed region in (b) of tdTomato-ABD2 fluorescence. (e) Intensity profiles of YFP-tubulin and tdTomato-ABD2 fluorescence along the X-Y axes in (c) and (d). These intensity profiles were obtained along manually selected lines. Scale bar indicates 10 μm.

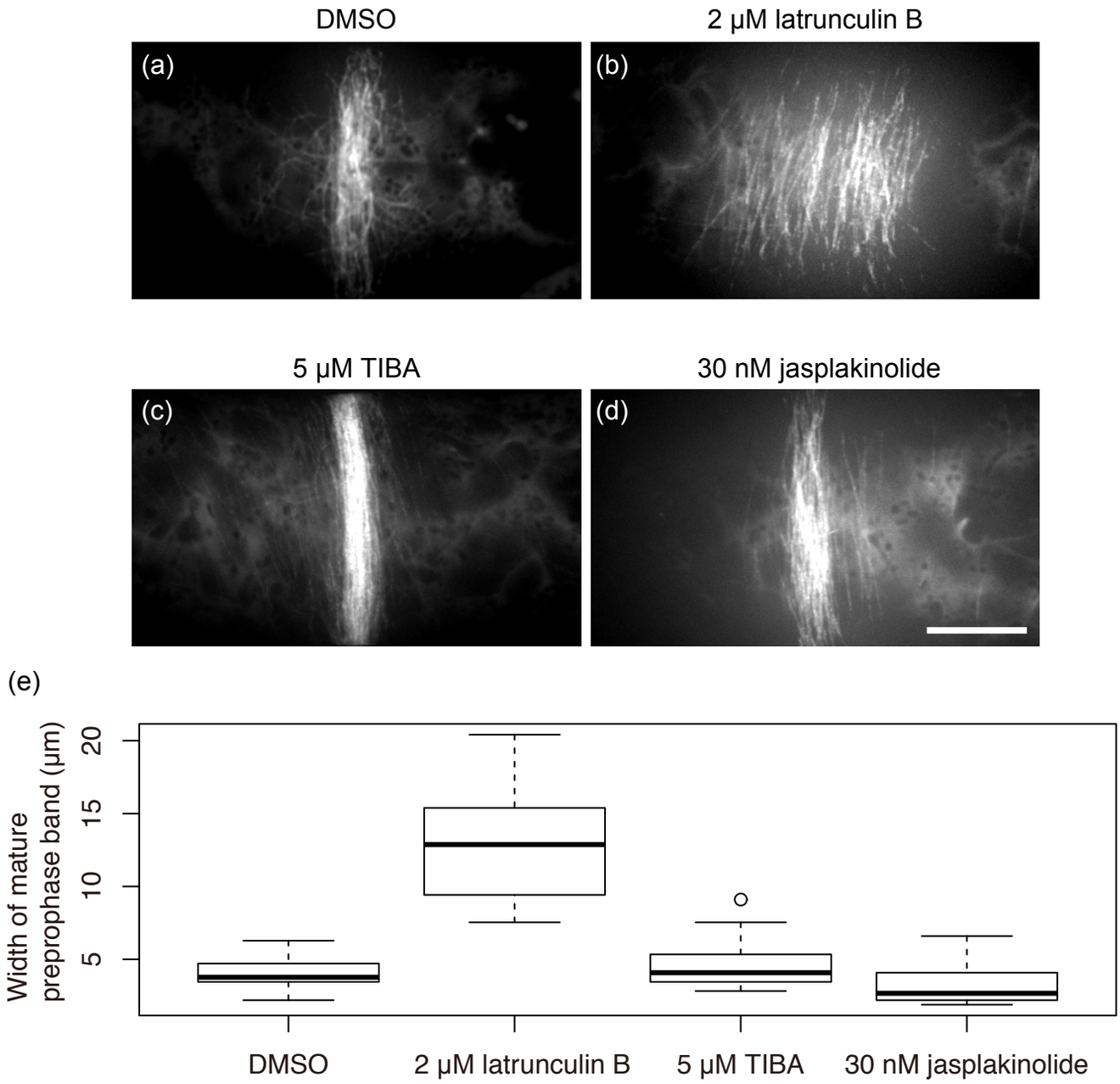

Figure 2. Effects of actin microfilaments inhibitors on preprophase band.

(a-d) Microtubules visualized in tobacco BY-2 cells stably expressing GFP-tubulin (BY-GT16 cells). Representative images of maximum intensity projections were constructed within a 0.5-μm step size. Cells treated with DMSO (a), 2 μM latrunculin B (b), 5 μM TIBA (c) or 30 nM Jasplakinolide (d) for 1 to 5 h. (e) A boxplot of preprophase band widths in cells treated with DMSO, latrunculin B, TIBA or jasplakinolide. The bottom and top of each box indicates the 25th and 75th percentiles. The maximum length of each whisker is 1.5 times the interquartile range (IQR), and data beyond the upper whisker are plotted using an empty circle. I measured 25 to 26 independent cells. Scale bar indicates 10 μm.

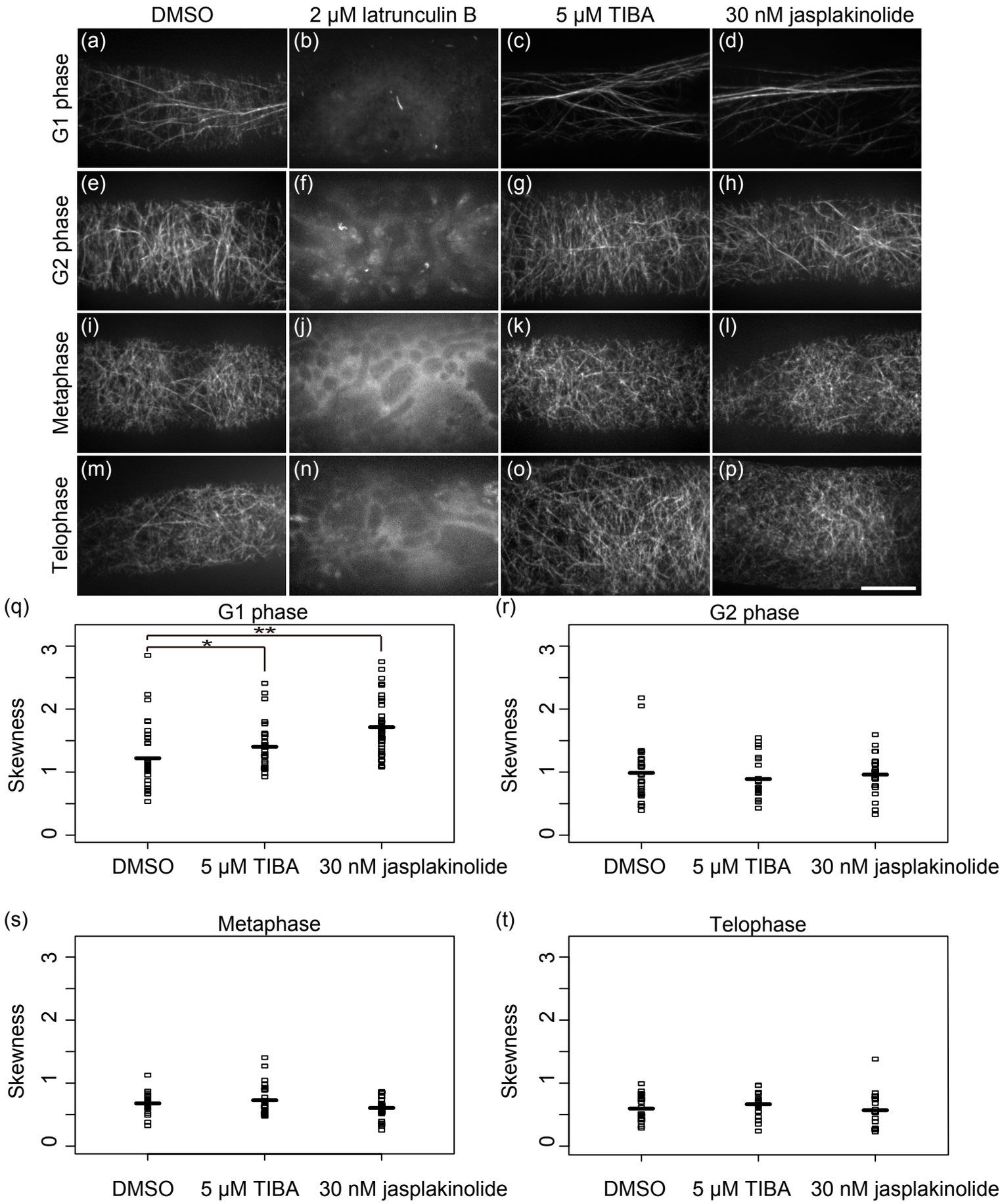
DMSO
2 μM latrunculin B
5 μM TIBA
30 nM jasplakinolide
G1 phase
G2 phase
Metaphase
Telophase
(a)
(b)
(c)
(d)
(e)
(f)
(g)
(h)
(i)
(j)
(k)
(l)
(m)
(n)
(o)
(p)
(q)
G1 phase
(r)
G2 phase
(s)
Metaphase
(t)
Telophase
Skewness
0
1
2
3
*
**
DMSO
5 μM TIBA
30 nM jasplakinolide

Figure 3. Effects of latrunculin B, TIBA and jasplakinolide on the cortical actin microfilament during cell cycle progression in BY-GF11 cells.

Actin microfilament structures labeled by GFP-ABD2 in tobacco BY-2 cells (BY-GF11 cells) at G1 (a-d), G2 (e-h), metaphase (i-l) and telophase (m-p). Representative images of maximum intensity projections were constructed from six serial optical sections within a 0.5-µm step size. Cell cycles were determined by position and morphology of the cell nuclei. Treatments with DMSO as control (a, e, i, m), 2 µM latrunculin B (b, f, j, n), 5 µM TIBA (c, g, k, o) or 30 nM jasplakinolide (d, h, l, p) for 2-4 h. Scale bar indicates 10 µm. (q-t) Skewness of GFP-ABD2 fluorescence intensity distribution in BY-GF11 cells treated with DMSO, 5 µM TIBA or 30 nM Jasplakinolide in G1 phase (q), G2 phase (r), metaphase (s) and telophase (t). Asterisk and double asterisk indicate significant differences ($P < 0.05$ and $P < 0.01$, respectively, u-test) between cells treated with DMSO and 5 µM TIBA or 30 nM jasplakinolide.

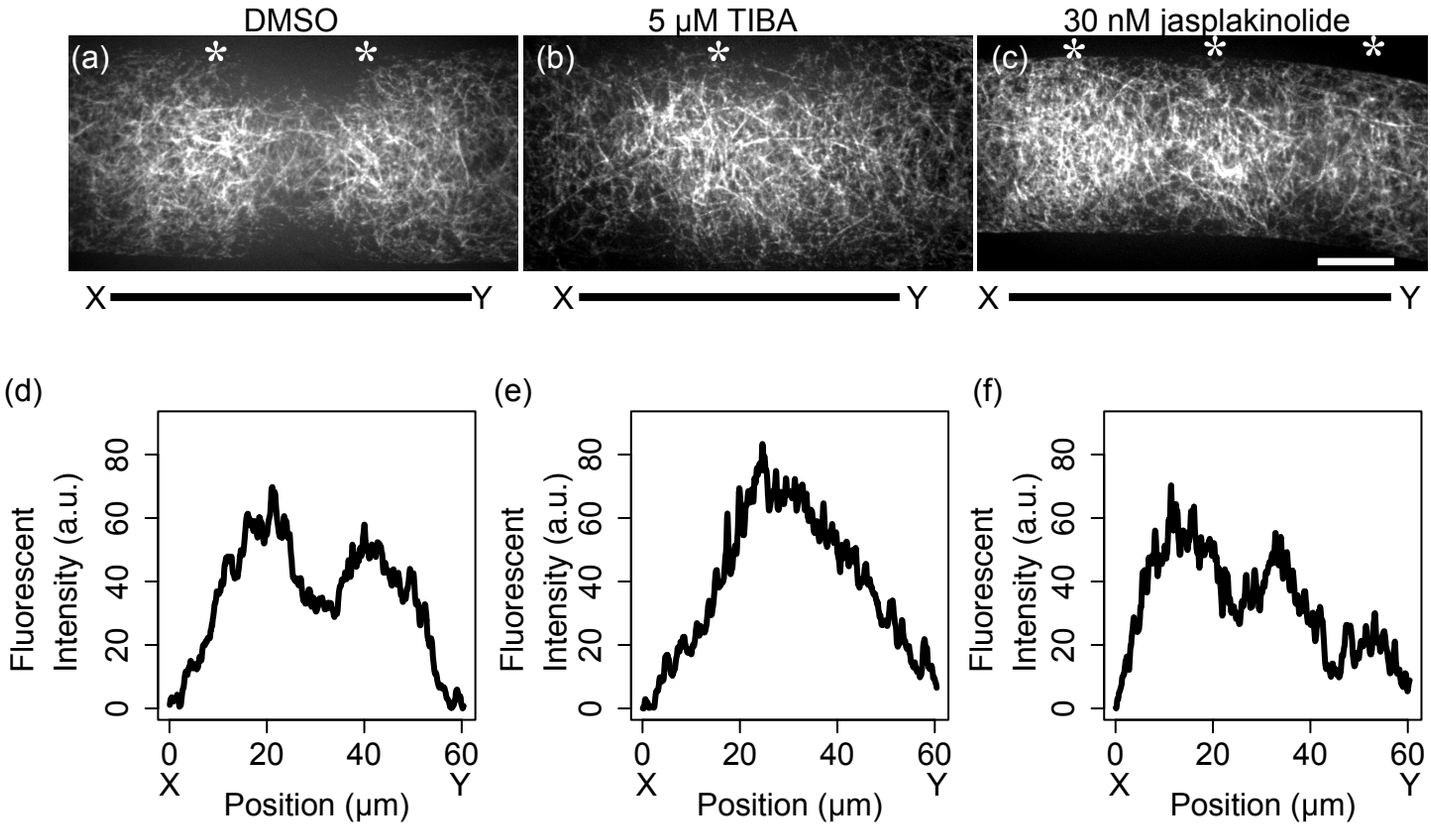

Figure 4. TIBA and jasplakinolide alter cortical actin microfilament patterning at metaphase in BY-GF11 cells. BY-GF11 cells treated with (a) DMSO, (b) 5 μM TIBA or (c) 30 nM jasplakinolide were observed at metaphase. Representative images of maximum intensity projections were constructed from serial optical sections within a 0.5-μm step size. Asterisks indicate the peaks of actin microfilament distribution. (d-f) Intensity profiles of GFP-ABD2 fluorescence along the X-Y axes in (a-c). These profiles were obtained by perpendicular signal averaging. Following treatment, two intensity peaks were observed with DMSO (d), 37% of cells showed one intensity peak with TIBA (e), and 32% of cells showed three intensity peaks with jasplakinolide (f). Scale bar indicates 10 μm. See also Table 1.

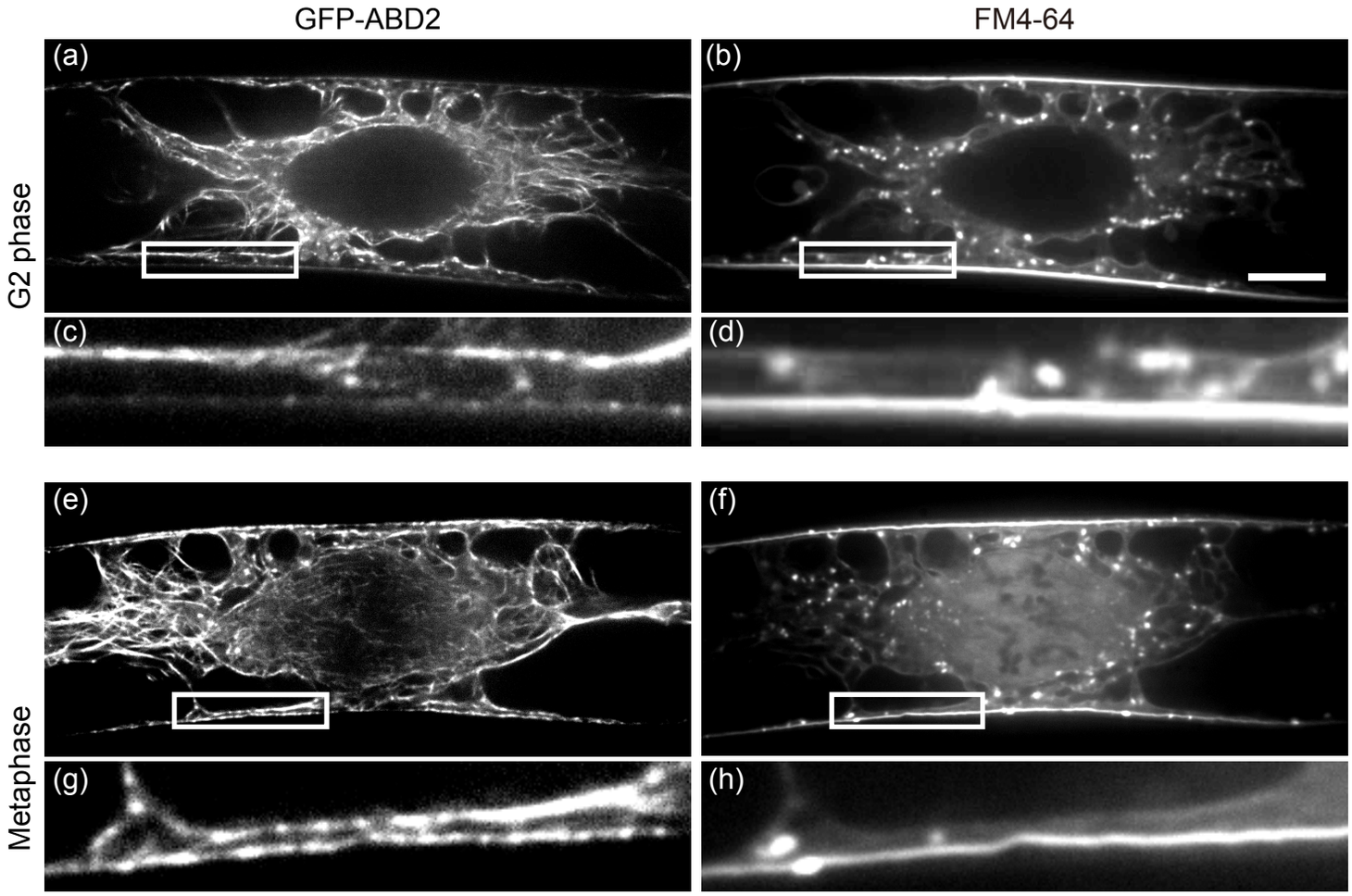
GFP-ABD2
FM4-64
(a)
(b)
(c)
(d)
(e)
(f)
(g)
(h)
G2 phase
Metaphase

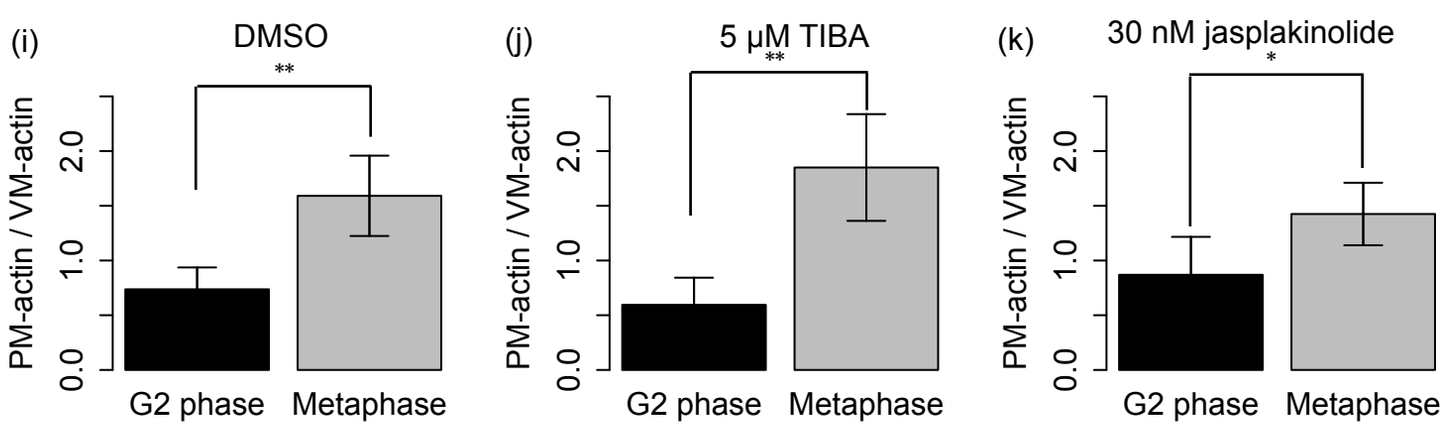
(i)
DMSO
**
PM-actin / VM-actin
0.0
1.0
2.0
G2 phase
Metaphase
(j)
5 μM TIBA
**
PM-actin / VM-actin
0.0
1.0
2.0
G2 phase
Metaphase
(k)
30 nM jasplakinolide
*
PM-actin / VM-actin
0.0
1.0
2.0
G2 phase
Metaphase

Figure 5. Detailed observations of actin microfilament, plasma membrane and vacuolar membrane visualized by GFP-ABD2 and FM4-64 at G2 and metaphase.

(a, b) Actin microfilaments labeled by GFP-ABD2 (a) and plasma membrane and vacuolar membrane stained by FM4-64 (b) at G2 phase. (c) Magnification of inset in (a). (d) Magnification of inset in (b). (e, f) Actin microfilaments labeled by GFP-ABD2 (e) and plasma membrane and vacuolar membrane stained by FM4-64 (f) at metaphase. (g) Magnification of inset in (e). (h) Magnification of inset in (f). (i-k) Ratio of GFP-ABD2 on the plasma membrane to that on the vacuolar membrane in BY-GF11 cells treated with DMSO (i), 5 μM TIBA (j) or 30 nM jasplakinolide (k). Note that the ratio increases from G2 phase to metaphase in DMSO control (i) as well as after treatment with TIBA (j) or jasplakinolide (k). Bars represent the standard deviations of six to 10 independent experiments. Asterisks and double asterisks indicate significant differences (***P*** < 0.05 and *P* < 0.01, respectively, t-test) between G2 phase and metaphase. Scale bars indicate 10 μm in (a, b, e, f) and 2 μm in (c, d, g, h) respectively.

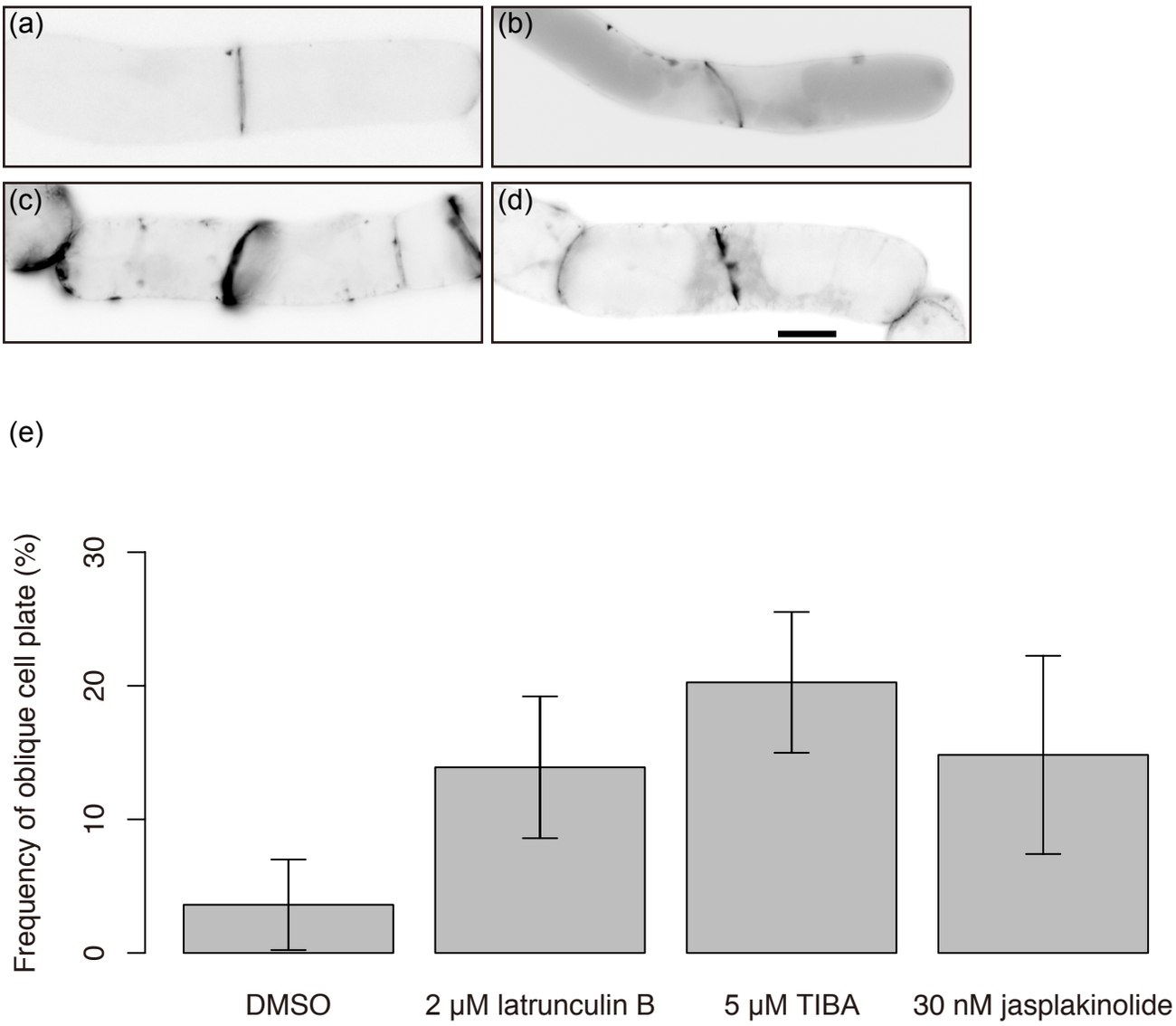

Figure 6. Effects of actin microfilament inhibitors on the orientation of the division plane in BY-2 cells.
(a-d) Representative images of division planes stained with aniline blue in BY-GF11 cells treated with DMSO (a), 2 μM latrunculin B (b), 5 μM TIBA (c) or 30 nM jasplakinolide (d) for 5 h. Inhibitors were added 5 h after aphidicolin removal. Just before aniline blue staining, cells were fixed with 3.7% formaldehyde.
(e) Frequencies of oblique cell plates with angles of more than 10 degrees against the cell short axis in cells treated with DMSO, latrunculin B, TIBA and jasplakinolide. I measured 185-326 independent planes. Bars represent the standard deviation. Scale bar indicates 10 μm.

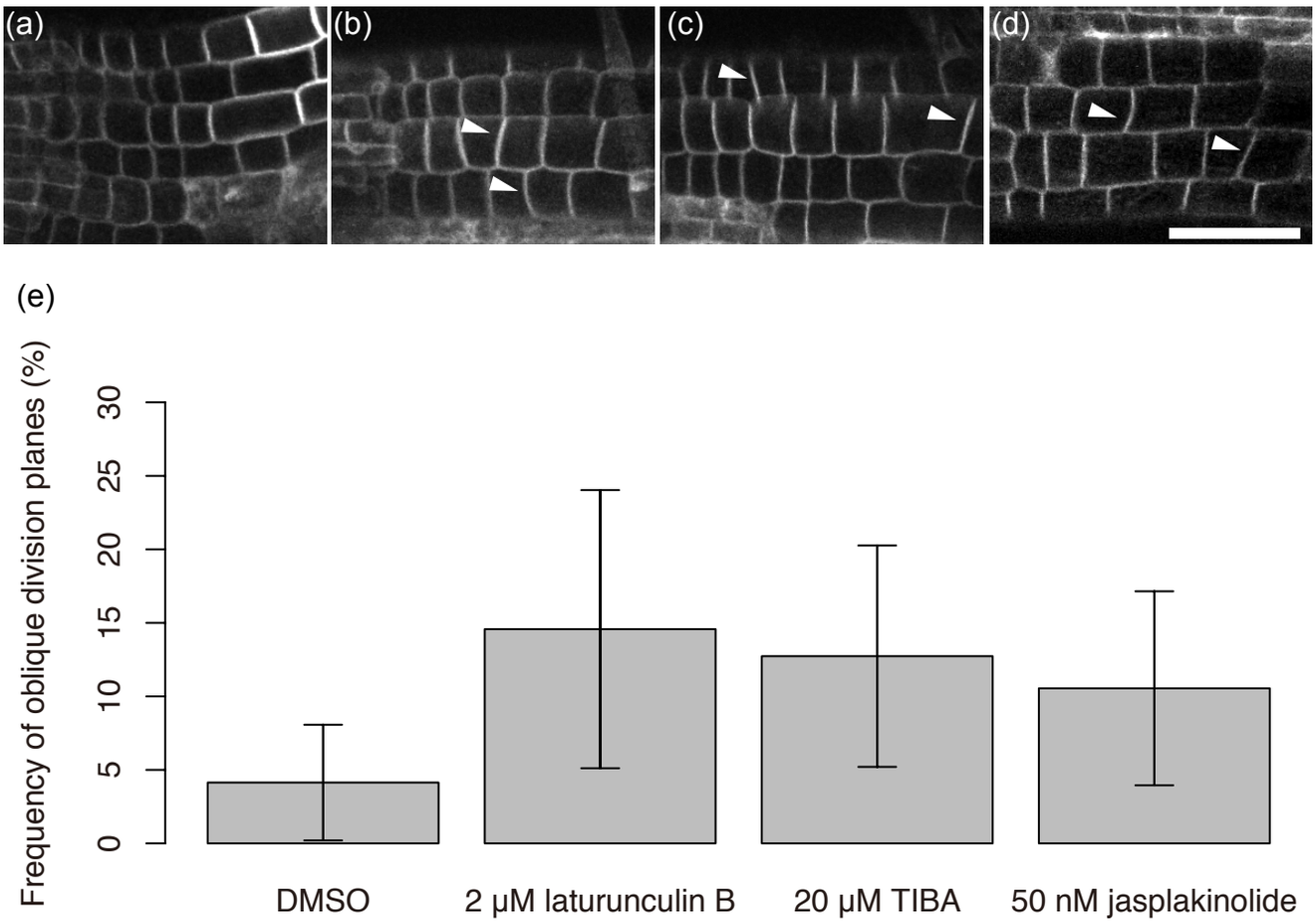

Figure 7. Effects of actin microfilament inhibitors on the orientation of the division plane in *Arabidopsis thaliana*.

(a-d) Representative images of 1-week-old GFP-PIP2a expressing *A*. *thaliana* root tip treated with DMSO (a), 2 μM latrunculin B (b), 20 μM TIBA (c) or 50 nM jasplakinolide (d) for 24 h. Oblique division planes were indicated by arrowhead. (e) Frequencies of oblique division planes with angles of more than 10 degrees against the root latitudinal axis in *A*. *thaliana* treated with DMSO, latrunculin B, TIBA or jasplakinolide. I measured 241-368 independent planes. Bars represent the standard deviation. Scale bar indicates 50 μm.

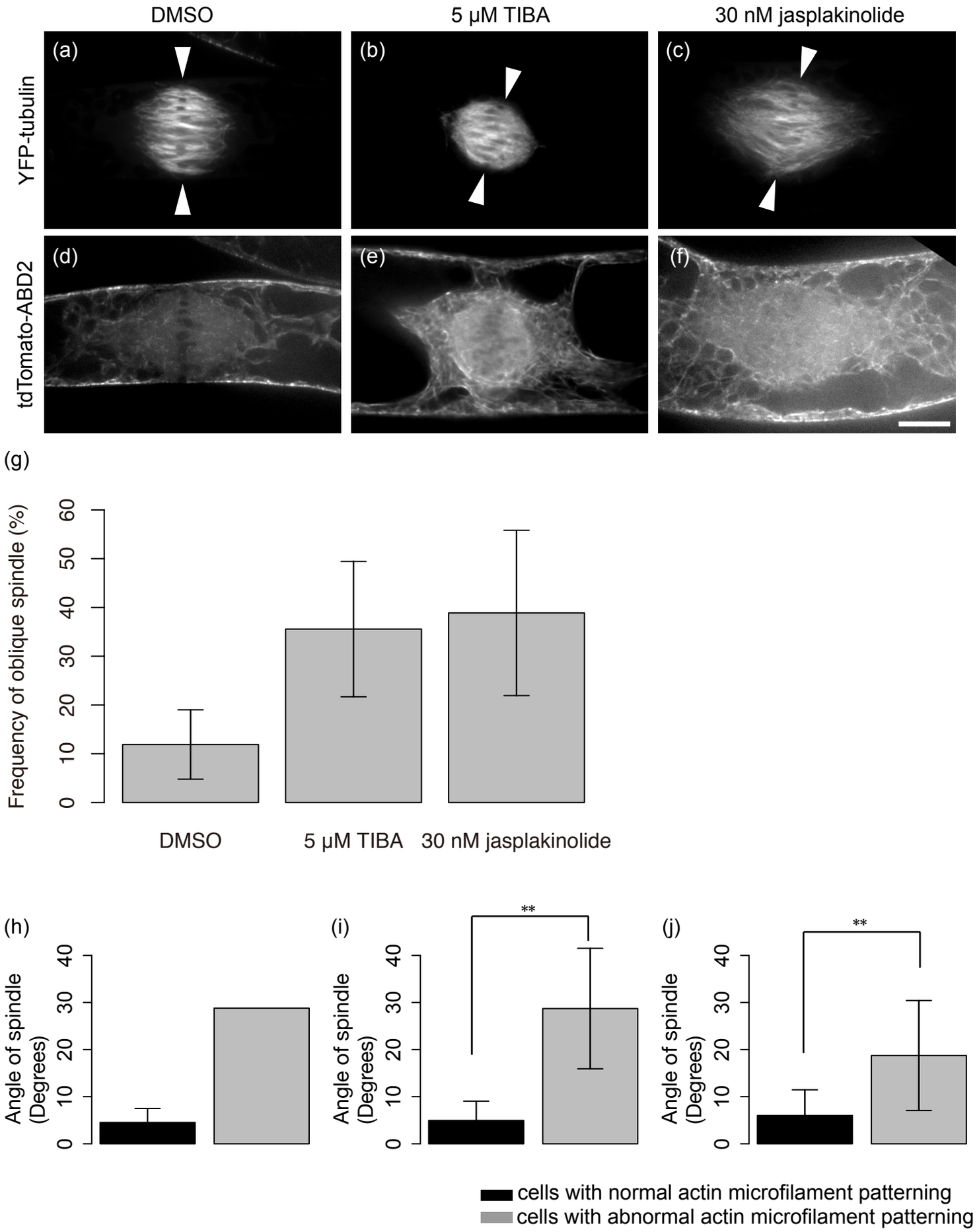
DMSO
5 μM TIBA
30 nM jasplakinolide
YFP-tubulin
tdTomato-ABD2
(a)
(b)
(c)
(d)
(e)
(f)
(g)
Frequency of oblique spindle (%)
0
10
20
30
40
50
60
DMSO
5 μM TIBA
30 nM jasplakinolide
(h)
(i)
(j)
Angle of spindle (Degrees)
0
10
20
30
40
**
cells with normal actin microfilament patterning
cells with abnormal actin microfilament patterning

Figure 8. Effects of TIBA and jasplakinolide on the spindle orientation in BY-YTRF1 cells.
(a-f) Microtubules labeled by YFP-tubulin (a-c) and actin microfilaments labeled by tdTomato-ABD2 (d-f) at metaphase in BY-YTRF1 cells treated with DMSO (a, d), 5 μM TIBA (b, e) or 30 nM jasplakinolide (c, f) for 2-3 h. Arrowheads indicate the equatorial planes. Inhibitors were added 5 h after aphidicolin removal. Cells treated with TIBA and jasplakinolide possessed altered cortical actin microfilament patterning with one intensity peak or three intensity peaks. Scale bar indicates 10 μm. (g) Frequency of oblique spindles with angles more than 10 degrees against the cell short axis in cells treated with DMSO, TIBA and jasplakinolide. Bars represent the standard deviation. (h-j) Mean angles of spindle orientation in BY-YTRF1 cells treated with DMSO (h), 5 μM TIBA (i) or 30 nM jasplakinolide (j). Black and gray boxes indicate the average angle of spindle orientation in cells with normal and abnormal cortical actin microfilament patterning, respectively, following DMSO (h), 5 μM TIBA (i) or 30 nM jasplakinolide (j) treatment. Double asterisks indicate significant differences ($P < 0.01$, t-test) between spindle orientation with normal and abnormal cortical actin microfilament patterning. Bars represent the standard deviation of 10-30 independent experiments. Because of low sample numbers (n=3), standard deviation of DMSO treated cells with altered actin microfilament patterning was not calculated.

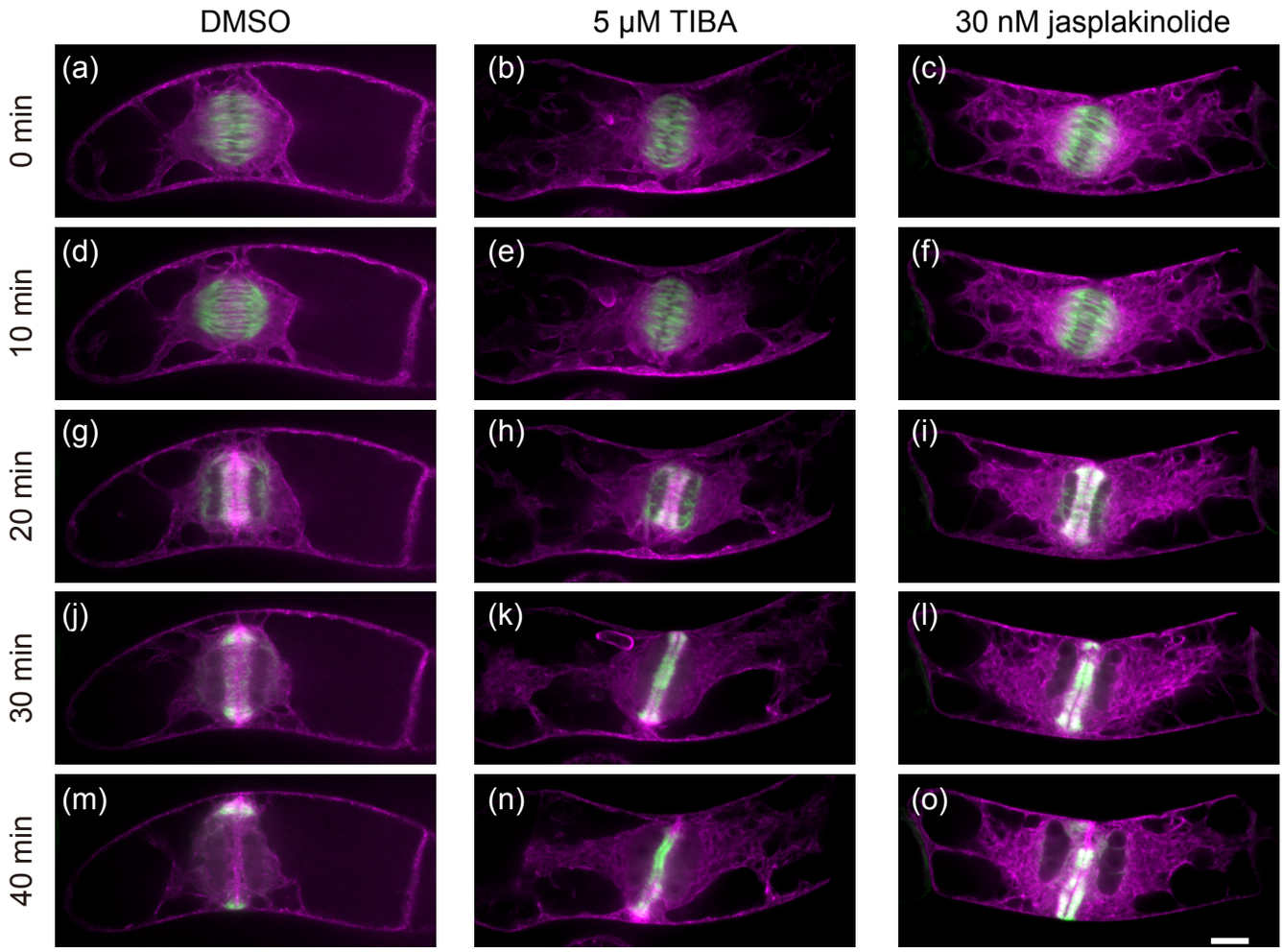

Figure 9. Time sequential observation of cortical actin microfilament patterning and division plane orientation in BY-YTRF1 cells.

Microtubules labeled by YFP-tubulin (green) and actin microfilaments labeled by tdTomato-ABD2 (magenta) from metaphase to telophase. Cells treated with DMSO (a, d, g, j, m), 5 μM TIBA (b, e, h, k, n) or 30 nM jasplakinolide (c, f, i, l, o) for 3 to 4 h. These data are representative images of 10-13 independent experiments. Scale bar indicates 10 μm.

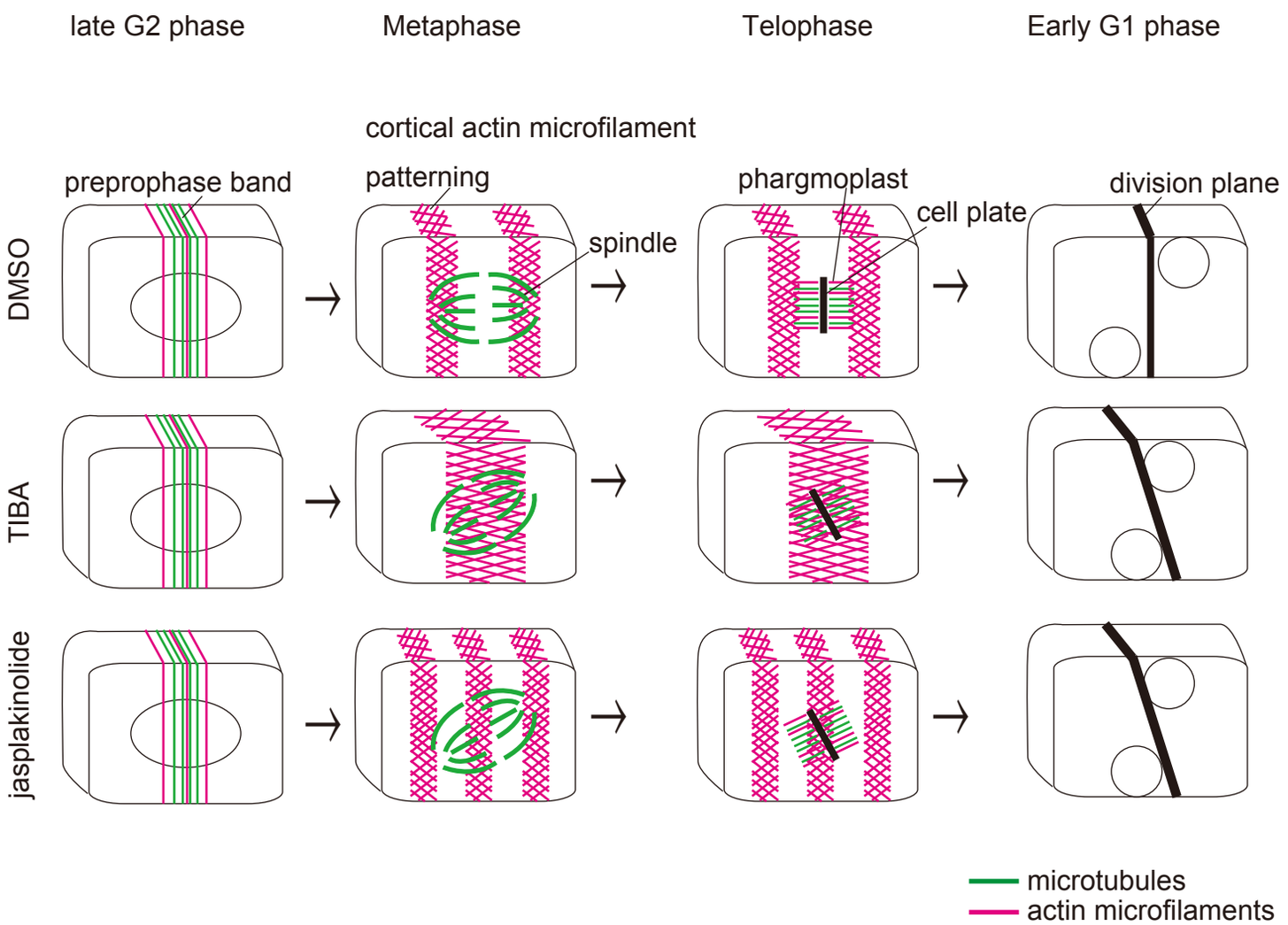

Figure 10. Schematic representation of effects of TIBA and jasplakinolide on cortical actin microfilaments and division plane orientation.

Abnormal cortical actin microfilament patterning is correlated with oblique division plane orientation.

	DMSO	5 μM TIBA	30 nM jasplakinolide
single peak	2.38 ± 4.12%	37.0 ± 17.3%	N. D.
twin peaks	90.1 ± 3.83%	53.3 ± 7.35%	68.5 ± 16.0%
triple peaks	7.54 ± 0.690%	9.70 ± 10.0%	31.5 ± 16.0%

Table 1. Effects of TIBA and jasplakinolide on the frequency of cortical actin microfilament patterns with single peak, twin and triple peaks at metaphase.

Cell cycle-synchronous BY-GF11 cells (5 h after aphidicolin removal) were treated with DMSO (n = 40), 5 μM TIBA (n = 32) or 30 nM jasplakinolide (n = 62) for 2-3 h. Data show the mean values and standard deviations. N.D. stands for Not Detected.

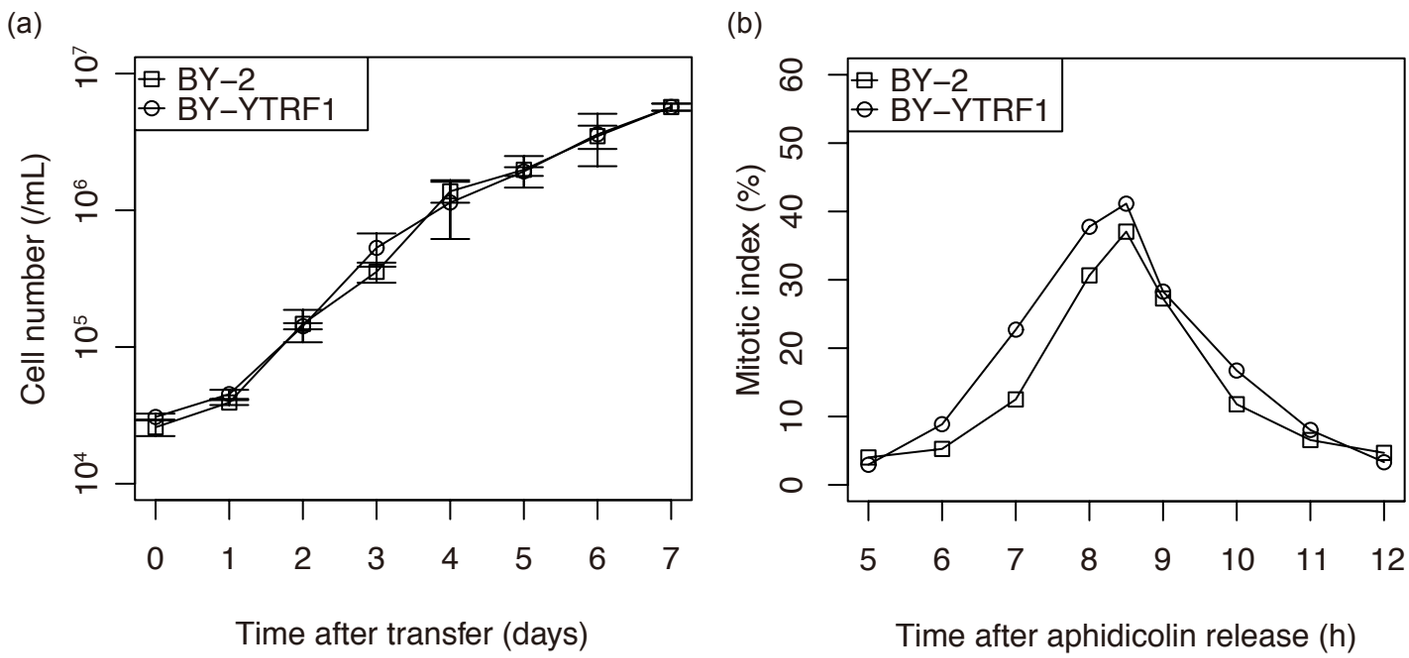

Supplemental Figure 1. Growth curve and change in mitotic index after release from aphidicolin treatment of original BY-2 and BY-YTRF1 cells.

(a) The growth curve of original BY-2 (open squares) and BY-YTRF1 (open circle) cells. The data in (a) shows the mean value ± SD of three independent experiments and the data in (b) shows each representative one.

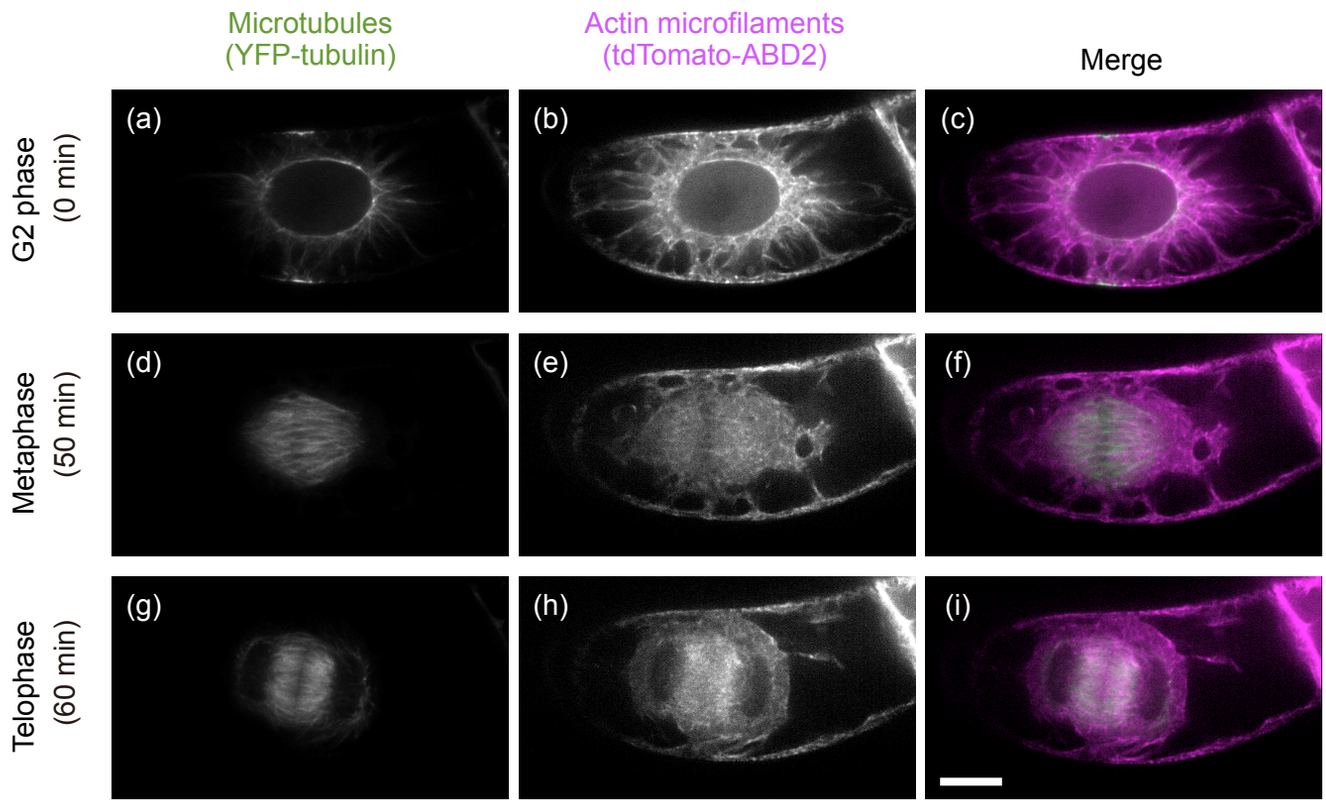

Supplemental Figure 2. Time sequential observations of microtubule and actin microfilament during cell cycle progression in BY-YTRF1 cells.

Microtubule visualized by YFP-tubulin (a, d, g) and actin microfilament visualized by tdTomato-ABD2 (b, e, h), and their merged images (c, f, i). Times are shown as 0, 50 and 60 min and indicate G2 phase (a-c), metaphase (d-f) and telophase (g-i), respectively. Scale bar indicates 10 μm.

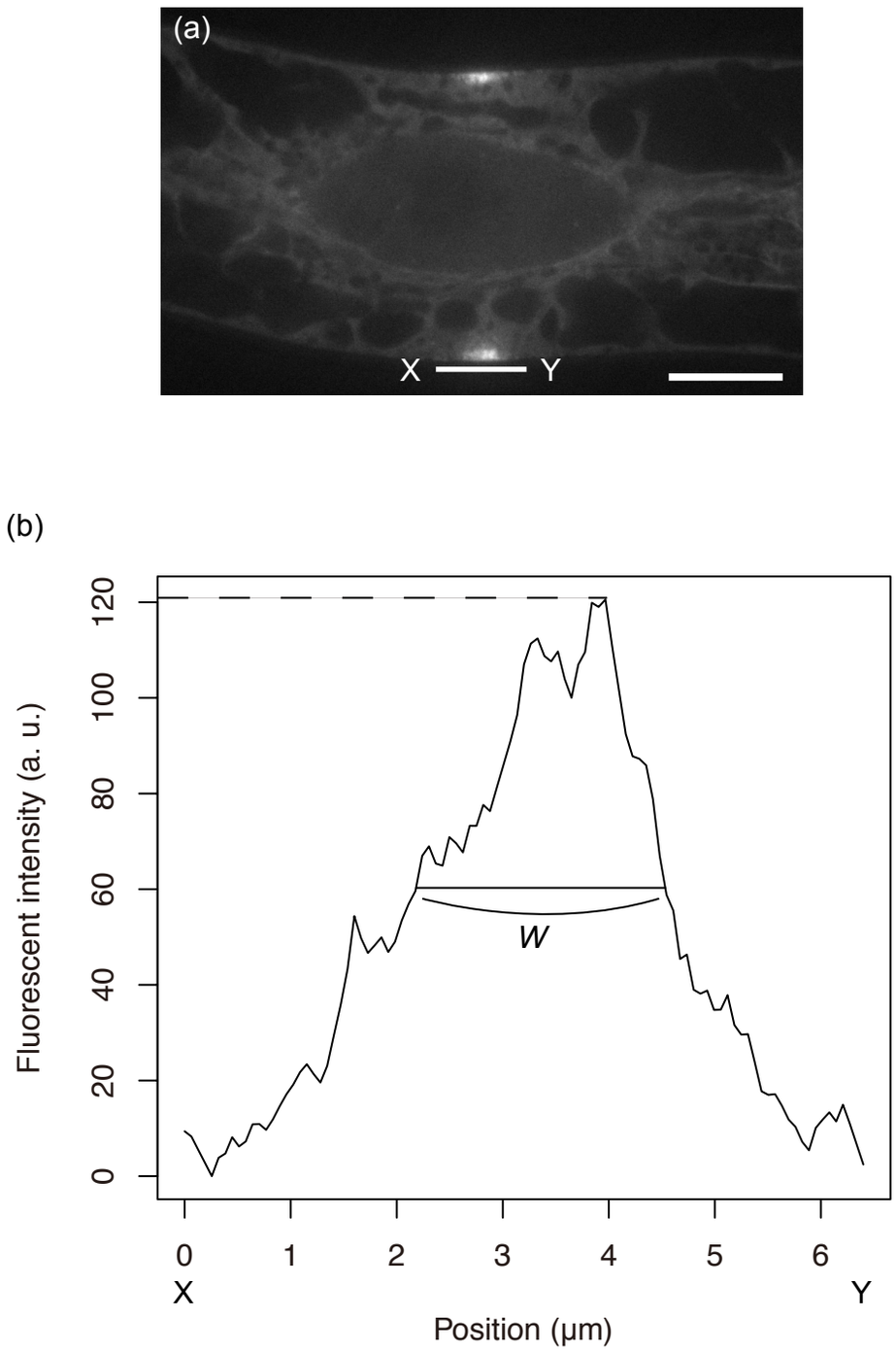

Supplemental Figure 3. Measurement of preprophase band width.

(a) Microtubule labeled by GFP-tubulin at prophase. (b) Intensity profiles of GFP-tubulin fluorescence along the X-Y axes in (a). Dashed line indicates maximum fluorescent intensity of GFP-tubulin. *W* indicates the full-width at half-maximum of the GFP-tubulin fluorescence profile and was defined as the width of the preprophase band.

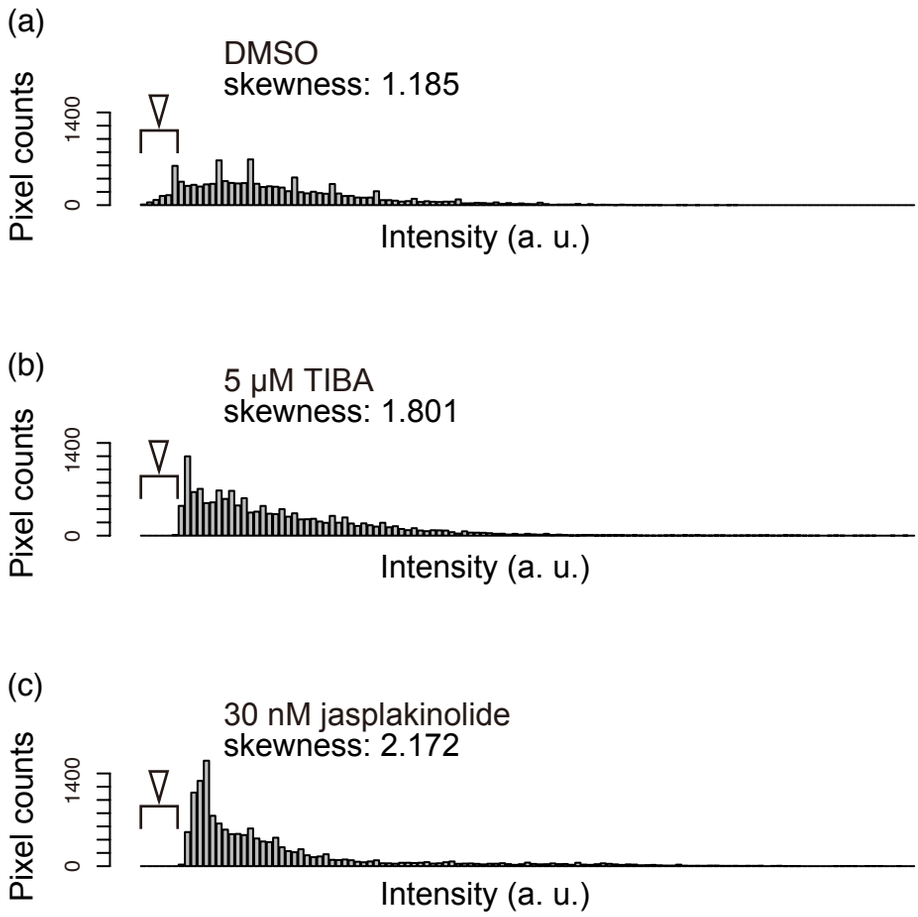

Supplemental Figure 4. Fluorescent intensity distribution of GFP-ABD2 in cells treated with DMSO (a), TIBA (b) and jasplakinolide (c) at G1 phase. The original fluorescence microscopic images are shown in Figure 3a, c and d, respectively. As the number of the low intensity pixels is decreased (arrowhead), the values of skewness increase in the cells treated with TIBA and jasplakinolide.

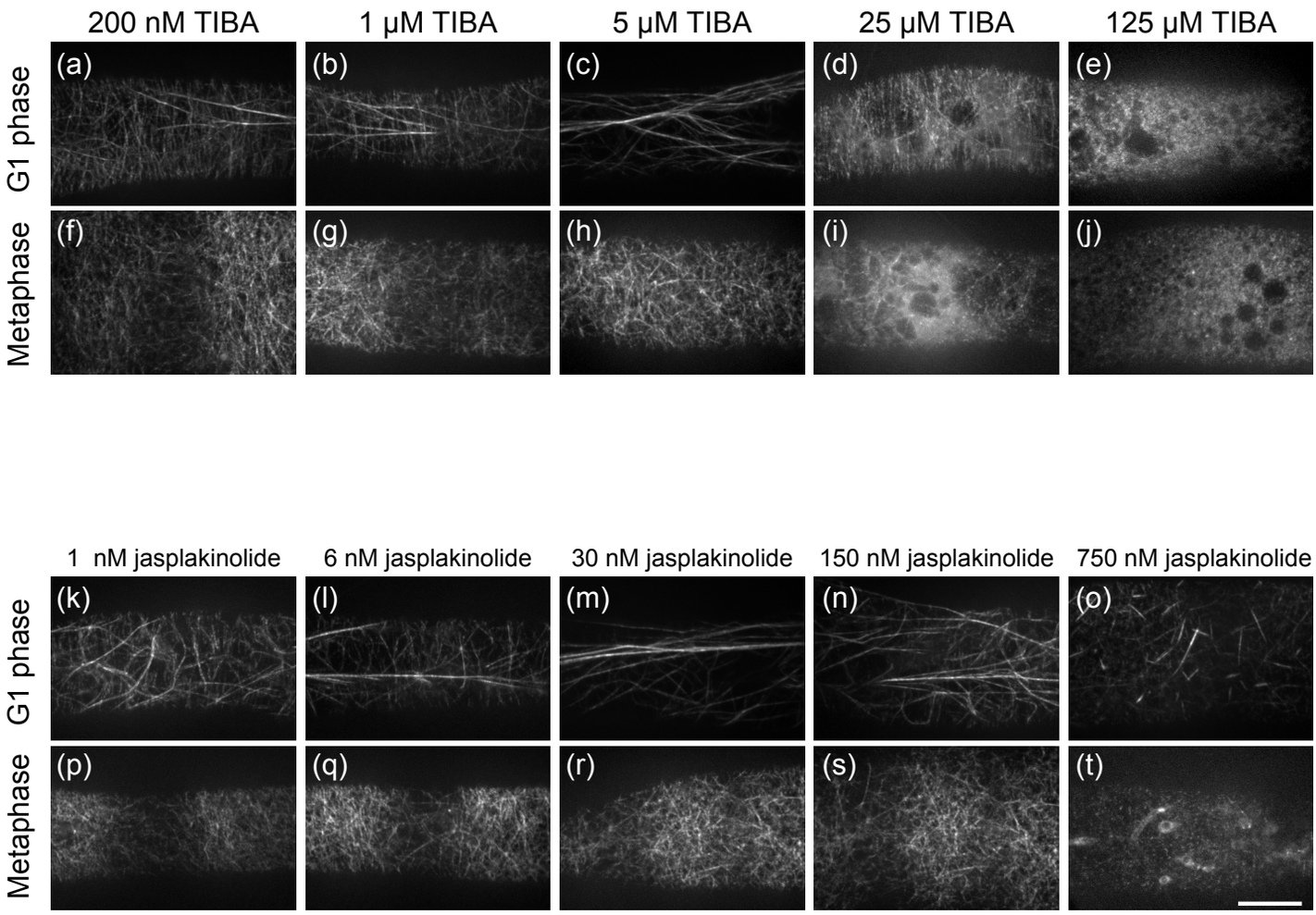

Supplemental Figure 5. Effects of several concentration of TIBA and jasplakinolide on the cortical actin microfilament at G1 phase and metaphase in BY-GF11 cells.

Actin microfilament structures labeled by GFP-ABD2 in BY-GF11 cells at G1 phase (a-e, k-o) and metaphase (f-j, p-t). Representative images of maximum intensity projections were constructed from six serial optical sections within a 0.5-μm step size. Cell cycles were determined by position and morphology of the cell nuclei. Treatments with 200 nM TIBA (a, f), 1 μM TIBA (b, g) , 5 μM TIBA (c, h), 25μM TIBA (d, i), 125μM TIBA (e, j), 1 nM jasplakinolide (k, p), 6nM jasplakinolide (l, q), 30 nM jasplakinolide (m, r), 150 nM jasplakinolide (n, s) or 750 nM jasplakinolide (o, t) for 2-4 h. For comparison, microscopic images of cells treated with 5 μM TIBA and 30 nM jasplakinolide at G1 phase and metaphase in Figure 3 (Fig. 3c, k, d, l) are used at (c), (h), (m) and (r), respectivety. Scale bar indicates 10 μm.

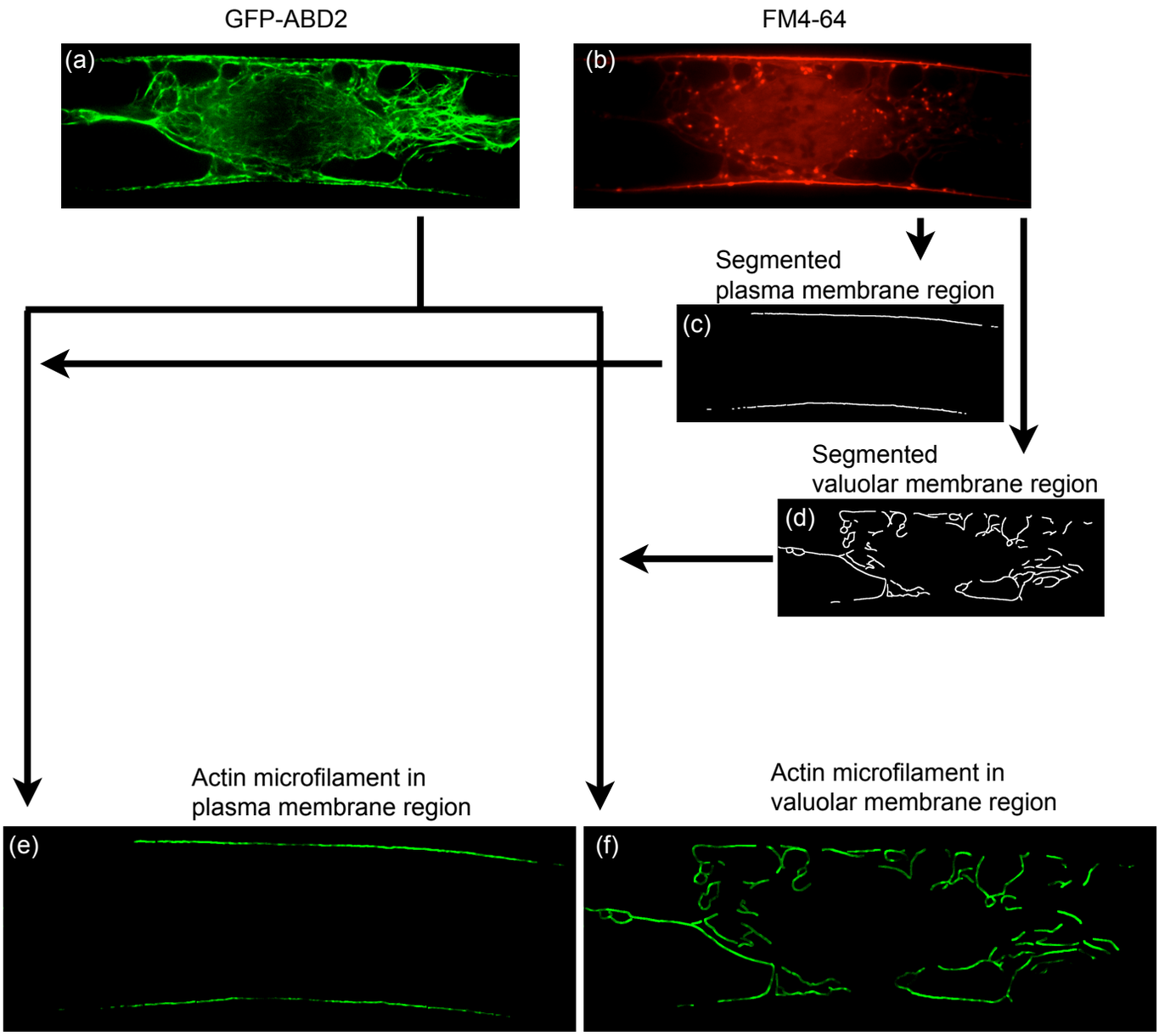

Supplemental Figure 6. Procedure for fluorescent intensity measurements of GFP-ABD2 associated with actin microfilament adjacent to the plasma membrane and vacuolar membrane.

To segment the actin microfilament adjacent to the plasma membrane and vacuolar membrane from the optical sections of GFP-ABD2 (a), I stained BY-GF11 cells with FM4-64, a tracing dye for the endocytic pathway. FM4-64 labeled the plasma membrane, endosomes and vacuolar membrane (b). Using the FM4-64 image, I then manually segmented the plasma membrane region (c) and vacuolar membrane region (d) as lines with a width of 0.064 µm (1 pixel). Actin microfilaments adjacent to the plasma membrane and vacuolar membrane were defined as the actin microfilament in the plasma membrane-region (e) and vacuolar membrane-region (f), respectively. I then measured the mean fluorescence intensity of the GFP-ABD2 adjacent to the plasma membrane and vacuolar membrane to calculate the intensity ratio (Fig. 5).

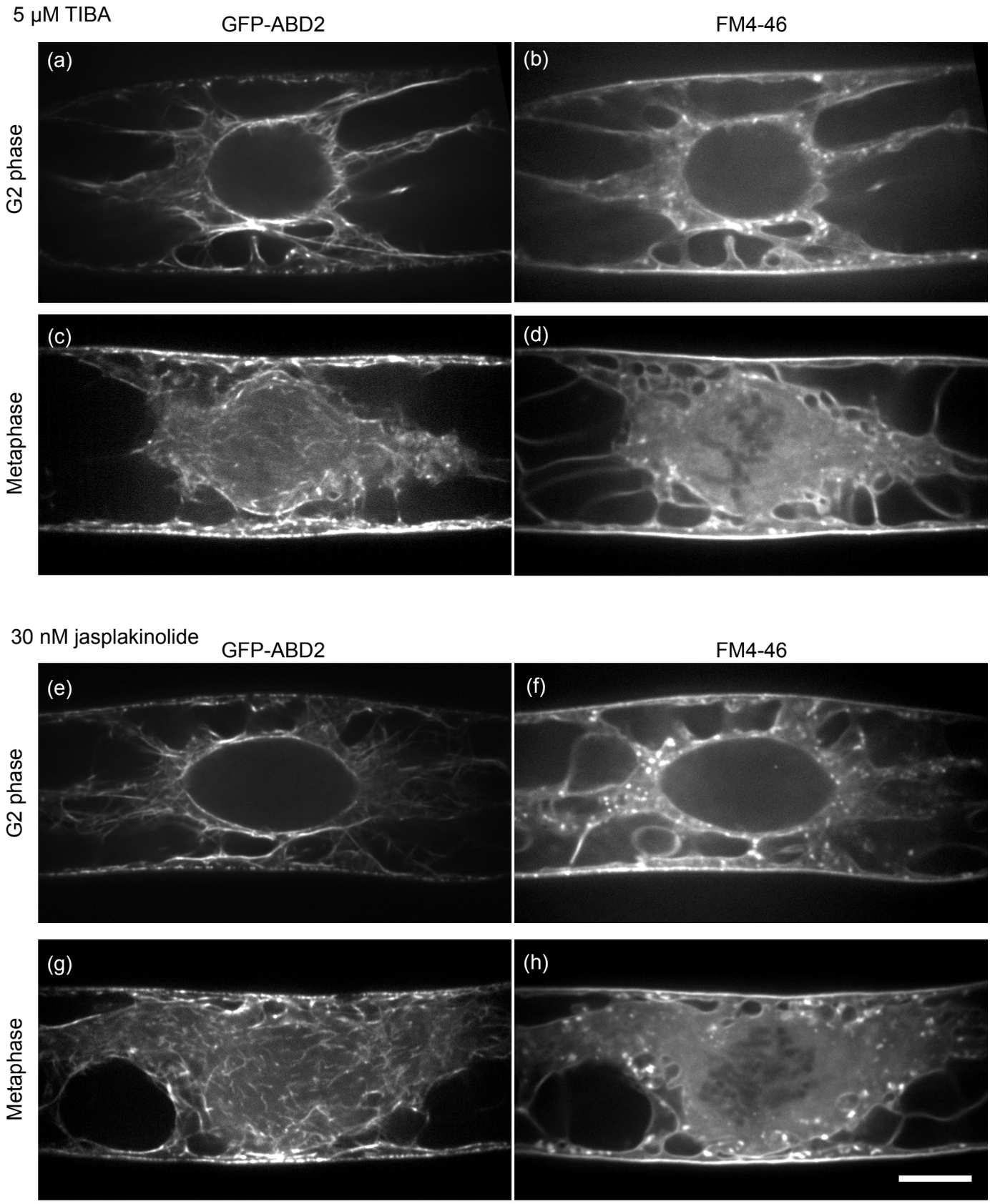

Supplemental Figure 7. Observation of actin microfilament, plasma membrane and vacuolar membrane labeled by GFP-ABD2 and FM4-64 in cells treated with TIBA and jasplakinolide at G2 and metaphase. Actin microfilament labeled by GFP-ABD2 (a, c, e, g) and plasma membrane and vacuolar membrane stained with FM4-64 (b, d, f, h) were observed at the G2 phase (a, b, e, f) and metaphase (c, d, g, h). The cells were treated with 2 μM TIBA (a-d) or 30 nM jasplakinolide (e-h). Scale bar indicates 10 μm.

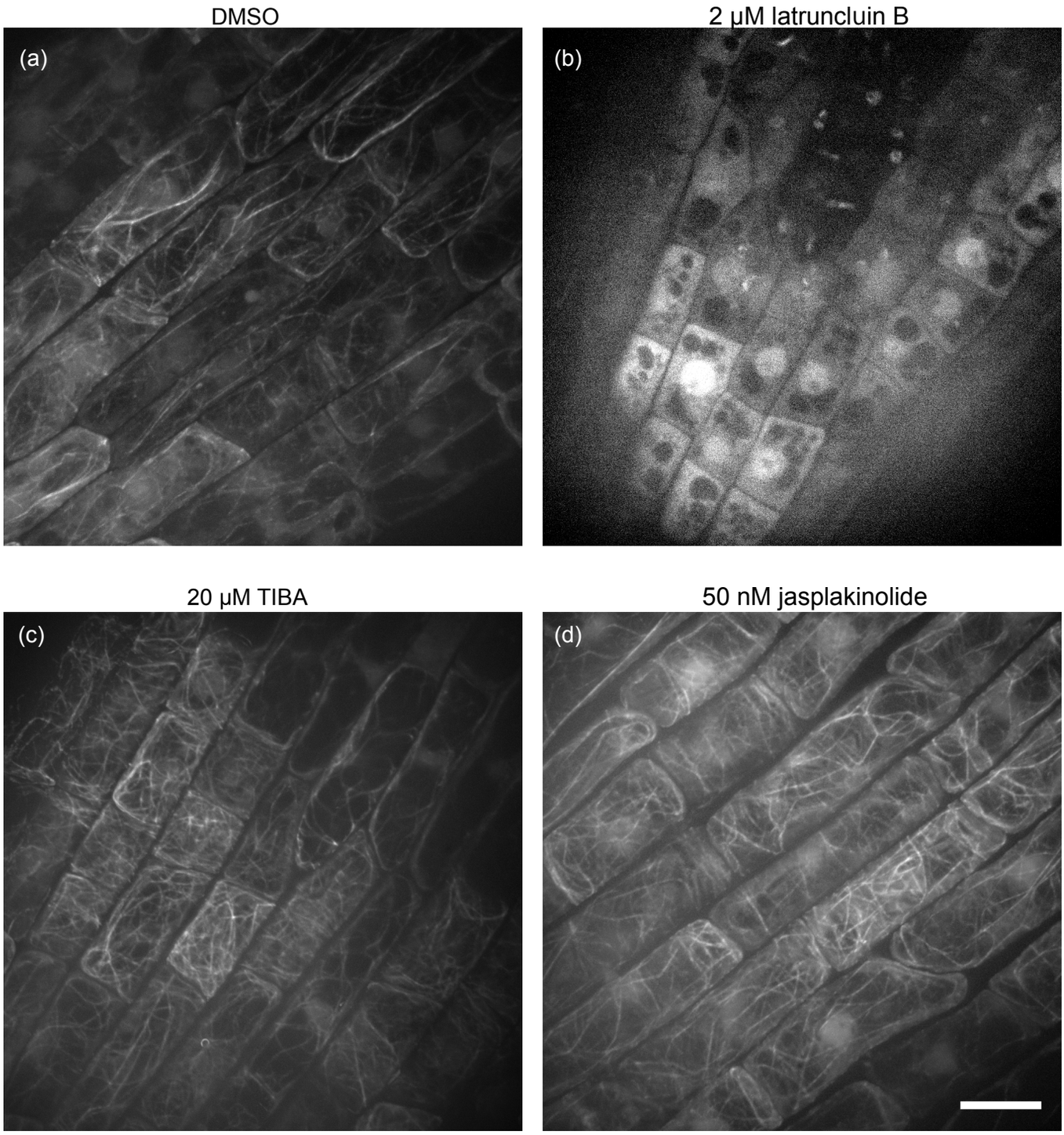

Supplemental Figure 8. Effects of actin microfilament inhibitors on the actin microfilament of *Arabidopsis thaliana* roots.

(a-d) Actin microfilament visualized by GFP-mTn in *A. thaliana* roots treated with DMSO (a), 2 μM latrunculin B (b), 20 μM TIBA (c) or 50 nM jasplakinolide (d). Scale bar indicates 10 μm.

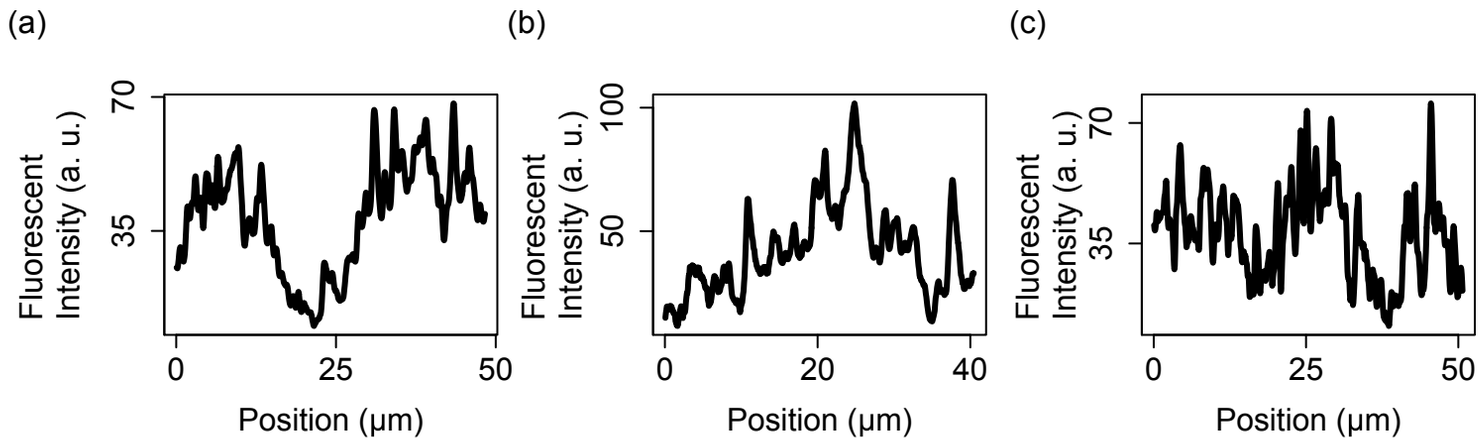

Supplemental Figure 9. Intensity profiles of tdTomato-ABD2 fluorescence along manually-selected cell cortex lines in BY-YTRF1 cells treated with DMSO (a), 5 μM TIBA (b) or 30 nM jasplakinolide (c) for 2-3 h. The original fluorescence microscopic images are shown in Figure 8d, e and f, respectively. Note that cells treated with TIBA or jasplakinolide possess one or three tdTomato-ABD2 intensity peaks, respectively, and cells treated with DMSO possess two normal intensity peaks.

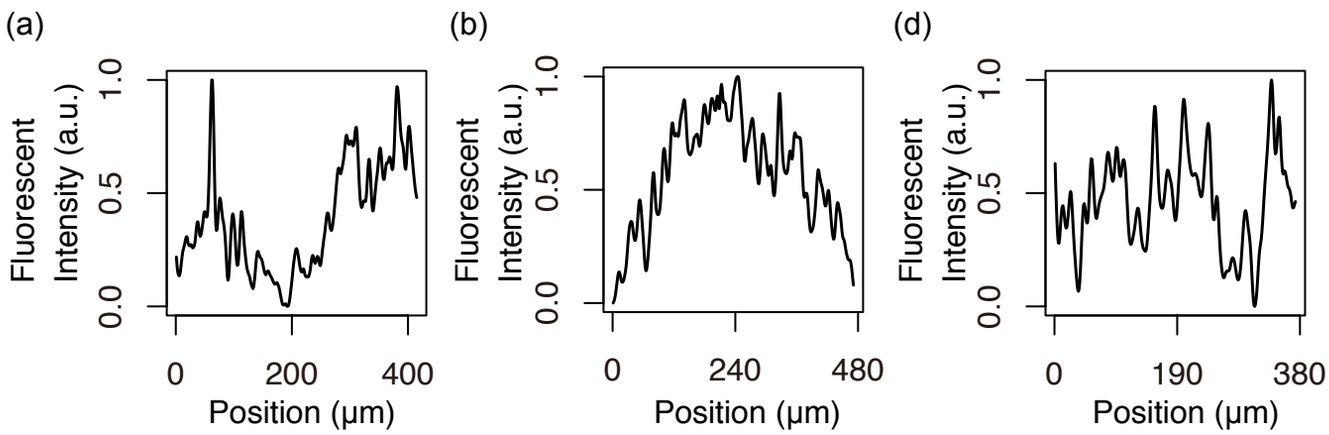

Supplemental Figure 10. Intensity profiles of tdTomato-ABD2 fluorescence along manually-selected cell cortex lines in BY-YTRF1 cells treated with DMSO (a), 5 μM TIBA (b) or 30 nM jasplakinolide (c) for 2-3 h. The original fluorescence microscopic images are shown in Figure 9a, b and c, respectively.

BY-2 cells

	observed cell plates	oblique cell plates
DMSO	278	13
2 μM latrunculin B **	242	34
5 μM TIBA **	326	64
30 nM jasplakinolide **	185	32

Arabidopsis root tip

	observed division planes	oblique division plates
DMSO	368	16
2 μM latrunculin B **	299	43
20 μM TIBA **	363	53
50 nM jasplakinolide **	241	30

** $P < 0.01$, *chi-square* test

Supplemental Table 1. Effect of latrunculin B, TIBA and jasplakinolide on cell plate and division plane orientation in BY-2 cells and *Arabidopsis* root tip. Double asterisks indicate significant differences ($P < 0.01$, *chi-square* test).

References

Abrámoff, M.D., Magalhães, P.J. and Ram, S.J. (2004) Image processing with ImageJ. *Biophotonics Int.* 11: 36-42.

Bubb, M.R., Senderowicz, A.M., Sausville, E.A., Duncan, K.L. and Korn, E.D. (1994) Jasplakinolide, a cytotoxic natural product, induces actin polymerization and competitively inhibits the binding of phalloidin to F-actin. *J. Biol. Chem.* 269: 14869-14871.

Chan, J., Calder, G., Fox, S. and Lloyd, C. (2005) Localization of the microtubule end binding protein EB1 reveals alternative pathways of spindle development in Arabidopsis suspension cells. *Plant Cell* 17: 1737-1748.

Cleary, A.L., Gunning, B.E.S., Wasteneys, G.O. and Hepler, P.K. (1992) Microtubule and F-actin dynamics at the division site in living *Tradescantia* stamen hair-cells. *J. Cell Sci.* 103: 977-988.

Dhonukshe, P., Grigoriev, I., Fischer, R., Tominaga, M., Robinson, D.G., Hašeki, J., Paciorek, T,. Petrášek, J., Seifertová, D., Tejos, R., Meisei, LA., Zažímalová, E., Gadella, T.W.Jr., Stierhof, Y.D., Ueda, T., Oiwa, K., Akhmanova, A., Brock, R., Spang, A. and Friml J. (2008) Auxin transport inhibitors impair vesicle motility and actin cytoskeleton dynamics in diverse eukaryotes. *Proc. Natl. Acad. Sci. USA* 105: 4489-4494.

Dhonukshe, P., Mathur, J., Hülskamp, M. and Gadella, T.W.Jr. (2005) Microtubule plus-ends reveal essential links between intracellular polarization and localized modulation of endocytosis during division-plane establishment in plant cells. *BMC Biol.* 3: 11.

Era, A., Tominaga, M., Ebine, K., Awai, C., Saito, C., Ishizaki, K., Yamato, K.T., Kochi, T., Nakano, A. and Ueda T. (2009) Application of Lifeact reveals F-Actin dynamics in *Arabidopsis thaliana* and the Liverwort, *Marchantia polymorpha*. *Plant Cell Physiol.* 50: 1041-1048.

Geldner, N., Friml, J., Stierhof, Y.D., Jürgens, G. and Palme, K. (2001) Auxin transport inhibitors block PIN1 cycling and vesicle trafficking. *Nature* 413: 425-428.

Granger, C. and Cyr, R. (2001) Use of abnormal preprophase bands to decipher division plane determination. *J. Cell. Sci.* 114: 599-607.

Higaki, T., Kutsuna, N., Okubo, E., Sano, T. and Hasezawa, S. (2006) Actin microfilaments regulate vacuolar structures and dynamics: dual observation of actin microfilaments and vacuolar membrane in living tobacco BY-2 cells. *Plant Cell Physiol.* 47: 839-852.

Higaki, T., Kutsuna, N., Sano, T. and Hasezawa, S. (2008) Quantitative analysis of changes in actin microfilament contribution to cell plate development in plant cytokinesis. *BMC Plant Biol.* 8: 80.

Higaki, T., Kutsuna, N., Sano, T., Kondo, N. and Hasezawa, S. (2010) Quantification and cluster analysis of actin cytoskeletal structures in plant cells: role of actin bundling in stomatal movement during diurnal cycles in Arabidopsis guard cells. *Plant J.* 61: 156-165.

Higaki, T., Sano, T. and Hasezawa, S. (2007) Actin microfilament dynamics and actin side-binding proteins in plants. *Curr. Opin. Plant Biol.* 10: 549-556.

Hoshino, H., Yoneda, A., Kumagai, F. and Hasezawa, S. (2003) Roles of actin-depleted zone and preprophase band in determining the division site of higher-plant cells, a tobacco BY-2 cell line expressing GFP-tubulin. *Protoplasma* 222: 157-165.

Kleine-Vehn, J., Dhonukshe, P., Swarup, R., Bennett, M. and Friml, J. (2006) Subcellular trafficking of the *Arabidopsis* auxin influx carrier AUX1 uses a novel pathway distinct from PIN1. *Plant Cell* 18: 3171-3181.

Kojo, KH., Higaki, T., Kutsuna, N., Yoshida, Y., Yasuhara, H. and Hasezawa, S. (2013) Roles of cortical actin microfilament patterning in division plane orientation in plants. *Plant Cell Physiol*. 54: 1491-1503.

Kumagai, F., Yoneda, A., Tomida, T., Sano, T., Nagata, T. and Hasezawa, S. (2001) Fate of nascent microtubules organized at the M/G1 interface, as visualized by synchronized tobacco BY-2 cells stably expressing GFP-tubulin: time-sequence observations of the reorganization of cortical microtubules in living plant cells. *Plant Cell Physiol.* 42: 723-732.

Kumagai-Sano, F., Hayashi, T., Sano, T. and Hasezawa, S. (2006) Cell cycle synchronization of tobacco BY-2 cells. *Nat. Protoc.* 1: 2621-2627.

Kutsuna, N. and Hasezawa, S. (2002) Dynamic organization of vacuolar and microtubule structures during cell cycle progression in synchronized tobacco BY-2 cells. *Plant Cell Physiol.* 43: 965-973.

Liu, B. and Palevitz, B.A. (1992) Organization of cortical microfilaments in dividing root-cells. *Cell Motil. Cytoskel.* 23: 252-264.

Lucas, J.R., and Sack, F.D. (2011) Polar development of preprophase bands and cell plates in the Arabidopsis leaf epidermis. *Plant J.* 69: 501-509.

Mineyuki, Y. (1999) The preprophase band of microtubules: Its function as a cytokinetic apparatus in higher plants. *Int. Rev. Cytol.* 187: 1-49.

Mineyuki, Y. and Palevitz, B.A. (1990) Relationship between preprophase band organization, F-actin and the division site in *Allium* - Fluorescence and morphometric studies on cytochalasin-treated Cells. *J. Cell Sci.* 97: 283-295.

Mongrand, S., Stanislas, T., Bayer, E.M., Lherminier, J. and Simon-Plas, F. (2010) Membrane rafts in plant cells. *Trends Plant Sci.* 15: 656-663.

Nagata, T., Nemoto, Y. and Hasezawa, S. (1992) Tobacco BY-2 cell line as the "HeLa" cell in the cell biology of higher plants. *Int. Rev. Cytol.* 132: 1-30.

Niedergang-Kamien, E. and Leopold, A.C. (1957) Inhibitors of polar auxin transport. *Physiol. Plant.* 10: 29-38.

Ou, G.S., Chen, Z.L. and Yuan, M. (2002) Jasplakinolide reversibly disrupts actin filaments in suspension-cultured tobacco BY-2 cells. *Protoplasma* 219: 168-175.

Panteris, E., Apostolakos, P. and Galatis, B. (2006) Cytoskeletal asymmetry in *Zea mays* subsidiary cell mother cells: a monopolar prophase microtubule half-spindle anchors the nucleus to its polar position. *Cell Motil. Cytoskel 63*: 696-709.

Panteris, E. (2008) Cortical actin filaments at the division site of mitotic plant cells: a reconsideration of the 'actin-depleted zone'. *New Phytol.* 179: 334-341.

Rasmussen, C.G., Sun, B. and Smith, L.G. (2010) Tangled localization at the cortical division site of plant cells occurs by several mechanisms. *J. Cell Sci.* 124: 270-279.

Rasmussen, C.G., Humphries, J.A. and Smith, L.G. (2011) Determination of symmetric and asymmetric division planes in plant cells. *Annu. Rev. Plant Biol. 62*: 387-409.

Saito, C., Morita, M.T., Kato, T. and Tasaka, M. (2005) Amyloplasts and vacuolar membrane dynamics in the living graviperceptive cell of the *Arabidopsis* inflorescence stem. *Plant Cell* 17: 548-558.

Sampathkumar, A., Lindeboom, J.J., Debolt, S., Gutierrez, R., Ehrhardt, D.W., Ketelaar, T., Persson, S. (2011) Live cell imaging reveals structural associations between the actin and microtubule cytoskeleton in *Arabidopsis*. *Plant Cell* 23: 2302-2313.

Sano, T., Higaki, T., Oda, Y., Hayashi, T. and Hasezawa, S. (2005) Appearance of actin microfilament 'twin peaks' in mitosis and their function in cell plate formation, as visualized in tobacco BY-2 cells expressing GFP-fimbrin. *Plant J.* 44: 595-605.

Snyder, W.E. (1949) Some responses of plants to 2,3,5-triiodobenzoic acid. *Plant Physiol.* 24: 195-206.

Spector, I., Braet, F., Shochet, N.R. and Bubb, M.R. (1999) New anti-actin drugs in the study of the organization and function of the actin cytoskeleton. *Microsc. Res. Tech.* 47: 18-37.

Valster, A.H., Pierson, E.S., Valenta, R., Hepler, P.K. and Emons, A.M.C. (1997) Probing the plant actin cytoskeleton during cytokinesis and interphase by profilin microinjection. *Plant Cell* 9: 1815-1824.

Voigt, B., Timmers, A.C.J., Samaj, J., Müller, J., Baluška, F. and Menzel, D. (2005) GFP-FABD2 fusion construct allows in vivo visualization of the dynamic actin cytoskeleton in all cells of Arabidosis seedlings. *Eur. J. Cell Biol*. 84: 595-608.

Walker, K.L., Müller, S., Moss, D., Ehrhardt, D.W. and Smith, L.G. (2007) *Arabidopsis* TANGLED identifies the division plane throughout mitosis and cytokinesis. *Curr. Biol.* 17: 1827-1836.

Wright, A.J., Gallagher, K. and Smith, L.G. (2009) discordia1 and alternative discordia1 function redundantly at the cortical division site to promote preprophase band formation and orient division planes in maize. *Plant Cell* 21: 234-247.

Xu, X.M., Zhao, Q., Rodrigo-Peiris, T., Brkljacic, J., He, C.S., Müller, S. and Meier, I. (2008) RanGAP1 is a continuous marker of the *Arabidopsis* cell division plane. *Proc. Natl. Acad. Sci. USA* 105: 18637-18642.

Yoneda, A., Akatsuka, M., Hoshino, H., Kumagai, F. and Hasezawa, S. (2005) Decision of spindle poles and division plane by double preprophase bands in a BY-2 cell line expressing GFP-tubulin. *Plant Cell Physiol.* 46: 531-538.